

Cosmology at the end of the world

Stefano Antonini^{1,*} and Brian Swingle^{1,2}

¹*Maryland Center for Fundamental Physics and Department of Physics, University of Maryland, College Park MD 20742, USA*

²*Condensed Matter Theory Center and Joint Center for Quantum Information and Computer Science, University of Maryland, College Park MD 20742, USA*

**Email: santonin@umd.edu*

May 11, 2022

Abstract

In the last two decades the Anti-de Sitter/Conformal Field Theory correspondence (AdS/CFT) has emerged as focal point of many research interests. In particular, it functions as a stepping stone to a still missing full quantum theory of gravity. In this context, a pivotal question is if and how cosmological physics can be studied using AdS/CFT. Motivated by string theory, braneworld cosmologies propose that our universe is a four-dimensional membrane embedded in a bulk five-dimensional AdS spacetime. We show how such a scenario can be microscopically realized in AdS/CFT using special field theory states dual to an “end-of-the-world brane” moving in a charged black hole spacetime. Observers on the brane experience cosmological physics and approximately four-dimensional gravity, at least locally in spacetime. This result opens a new path towards a description of quantum cosmology and the simulation of cosmology on quantum machines.

Contents

1	Introduction	2
2	Euclidean analysis	4
3	Lorentzian analysis and braneworld cosmology	6
4	Gravity localization	7
5	Discussion	10
	Acknowledgements	11

A	Euclidean action and Einstein-Maxwell equations	11
B	Euclidean analysis - details	13
C	Action comparison	16
D	Lorentzian analysis and braneworld cosmology - details	21
E	Gravity Localization and trapping coefficient method	24
E.1	TT perturbations and Schrödinger equation	25
E.2	Trapping coefficient method	28
E.3	Numerical results	30
E.4	Time scales and adiabatic approximation	35
	References	36

1 Introduction

The achievement of a quantum mechanical description of spacetime is one of the most challenging issues facing modern physics. The Anti-de Sitter/Conformal Field Theory (AdS/CFT) correspondence provides a promising starting point to accomplish this goal. As a concrete realization of the holographic principle,^{1,2} it relates the observables of a full quantum gravity theory living in a $(d+1)$ -dimensional spacetime (the bulk) to those of a d -dimensional dual field theory without gravity associated to the boundary of the bulk spacetime.³ However, at this stage AdS/CFT must still be regarded as a toy model of the physical world, since the asymptotically AdS spacetimes it describes are different from the universe we observe. In this paper we exhibit a viable way to study certain Friedmann-Lemaître-Robertson-Walker (FLRW) cosmologies using the AdS/CFT correspondence, realizing a recently proposed new perspective on braneworld cosmology and quantum gravity in a cosmological universe.⁴

AdS/CFT associates different states of the CFT to different geometries of the bulk spacetime. In particular, certain highly excited pure states of the CFT have a dual geometry hosting a black hole and a dynamical end-of-the-world (ETW) brane.⁵⁻⁹ This bulk configuration is built from a two-sided wormhole spacetime by replacing the left boundary with the ETW brane (see Figure 1). The original wormhole spacetime describes an entangled state of two CFTs, and the ETW brane corresponds to a complete measurement of one CFT to leave a pure state of the remaining CFT. Hence, observables in the CFT must probe the physics behind the horizon of the black hole, including the remaining part of the left asymptotic region¹⁰⁻¹³ and the evolution of the ETW brane.^{4,14}

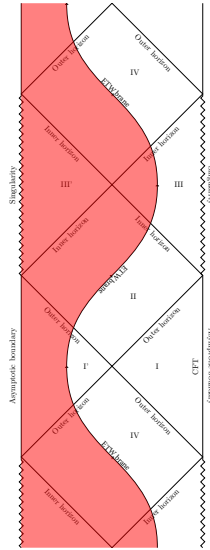


Figure 1: **Brane trajectory.** Maximally extended Penrose diagram for the AdS-Reissner-Nordström black hole. Only the time and radial directions are represented, while the other spatial dimensions are suppressed. Light rays move at an angle of 45° . More patches of the AdS-RN spacetime are glued together here. The ETW brane oscillates inside and outside the two horizons of the black hole, cutting off the left asymptotic region. The red region, generally part of the maximally extended charged black hole, is not present in our spacetime.

The presence of the brane opens an interesting scenario: when the bulk spacetime is 5-dimensional, an observer living on the 4-dimensional ETW brane would interpret the motion of the brane as the evolution of a FLRW universe, where the radial position plays the role of the scale factor.^{15–20} Hence, holographic duality allows to describe such “braneworld cosmologies” using CFT observables associated with the right asymptotic region of the black hole.⁴ Holographic cosmologies have been considered previously,^{21–23} also in the context of de Sitter holography²⁴ and braneworld holography.^{18–20,25} However, in the latter cases the holographic CFT lives on the brane and is coupled to gravity, whereas we are proposing a non-perturbative CFT description of the entire spacetime including the brane.

Now, a braneworld cosmological model can only be realistic if, for an observer living on the brane, gravity is effectively 4-dimensional and localized on the brane. The Randall-Sundrum model^{26,27} provides a mechanism for gravity localization on 4-dimensional branes embedded in AdS_5 bulk, and the mechanism can be generalized to different brane geometries²⁸ and to the presence of black holes.^{29,30} If the brane is not too close to the black hole horizon, gravity is localized, but only locally in spacetime: an experimentalist on the brane would observe ordinary gravity only on non-cosmological scales, and for a limited range of time. In this work we show that, in the presence of a charged black hole in the bulk (AdS-Reissner-Nordström),^{31–36} such gravity localization

is achievable without losing the dual CFT description of the spacetime. This proof-of-principle result, not attainable in the simplest setup of an AdS-Schwarzschild black hole and a pure tension brane,⁴ opens the door to a new formulation of cosmology within AdS/CFT. Our choice of units is $\hbar = c = \varepsilon_0 = k_B = 1$.

2 Euclidean analysis

The spacetime described above is dual to a CFT state that can be prepared in principle using a quantum computer. Theoretically, it is convenient to describe it starting from a Euclidean path integral. Extending previous works,^{4,37} the dual state is a fixed charge boundary state of the CFT on a spatial sphere S^{d-1} evolved for an imaginary (Euclidean) preparation time τ_0 :

$$|\Psi\rangle = e^{-\tau_0 H} |B, Q\rangle. \quad (1)$$

The ETW brane is associated to the past boundary condition in the path integral. In order to have a well defined CFT state and a sensible Euclidean geometry (see Figure 2), τ_0 must be positive.⁴

In Euclidean signature, the brane is the bulk extension of the CFT boundary.^{4,6,7} Its trajectory starts at the asymptotic boundary $r = \infty$ at $\tau = -\tau_0$, reaches a minimum radius $r = r_0$ and ends again on the boundary at $\tau = \tau_0$. Because the state is highly excited, the bulk geometry will also typically contain a black hole. The total Euclidean periodicity is given by the inverse temperature β of the black hole, determined by its size and charge. The brane trajectory excises part of this total range of Euclidean time, leaving only the interval $[-\tau_0, \tau_0]$ where the CFT is defined. Thus, the preparation time is determined by $2\tau_0 = \beta - 2\Delta\tau$, where $\Delta\tau$ is the total Euclidean time needed for the brane to cover half of its trajectory.

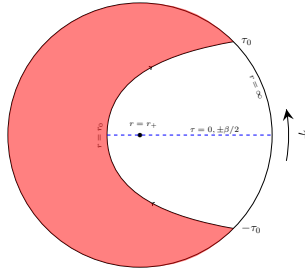


Figure 2: **Euclidean brane trajectory.** The Euclidean path integral on this spacetime computes the norm of the CFT state. The red region is cut off by the ETW brane.

The bulk physics is specified by the Euclidean action, which for the Einstein-Maxwell system considered here is $I = I_{bulk} + I_{ETW}$. I_{bulk} is the Einstein-Maxwell action with a negative cosmological constant $\Lambda = -d(d-1)/(2L_{AdS}^2)$, including a Gibbons-Hawking-York term and an electromagnetic boundary term (needed if the charge is held fixed³⁸⁻⁴⁰)

for the asymptotic boundary. The brane action reads:

$$I_{ETW} = -\frac{1}{8\pi G} \int_{ETW} d^d x \sqrt{h} [K - (d-1)T] + I_{ETW}^{em}, \quad (2)$$

where G is the d -dimensional Newton constant, K is the trace of the extrinsic curvature of the brane, T is the tension, h is the determinant of the metric induced on the brane and I_{ETW}^{em} is an electromagnetic boundary term. The variation of the bulk action leads to the Einstein-Maxwell equations with a negative cosmological constant, whose solution is the AdS-Reissner-Nordström (AdS-RN) metric (in Euclidean signature):

$$ds^2 = f(r)d\tau^2 + \frac{dr^2}{f(r)} + r^2 d\Omega_{d-1}^2 \quad (3)$$

with (for $d > 2$)

$$f(r) = 1 + \frac{r^2}{L_{AdS}^2} - \frac{2\mu}{r^{d-2}} + \frac{Q^2}{r^{2(d-2)}} \quad (4)$$

where μ and Q are the mass and charge parameters of the black hole. They can be expressed as a function of the inner (Cauchy) and outer (event) horizons of the black hole, solutions of the equations $f(r_+) = f(r_-) = 0$. The black hole is called extremal when $r_- = r_+$, corresponding to the maximum admissible charge for a fixed mass.

Varying the brane action, the equation

$$K_{ab} - Kh_{ab} = (1-d)Th_{ab} \quad (5)$$

is obtained, with $a, b = 0, \dots, d-1$. By parameterizing the trajectory of the brane with $r = r(\tau)$, equation (5) yields

$$\frac{dr}{d\tau} = \pm \frac{f(r)}{Tr} \sqrt{f(r) - T^2 r^2} \quad (6)$$

where the sign depends on if the brane is expanding or contracting. For $d > 2$ and $T < T_{crit} = 1/L_{AdS}$, a numerical evaluation gives two solutions for the equation $f(r) = T^2 r^2$, corresponding to the minimum radius of the brane: $r_0^+ > r_+$ and $r_0^- < r_-$. Between the two solutions the square root takes imaginary values. Since the brane is contracting from and expanding to $r = \infty$, the minimum radius is $r_0 = r_0^+$. The role of the solution r_0^- will be clear later.

Given values of d , r_+ , r_- and T , it is possible to evaluate the Euclidean time $\Delta\tau$ and therefore the preparation time τ_0 . We find that, for a black hole sufficiently close to extremality, i.e. for $r_- \rightarrow r_+$, it is possible to approach the critical value of the tension T_{crit} while retaining a sensible Euclidean solution, i.e. with $\tau_0 > 0$. At the same time, when $T \rightarrow T_{crit}$ the ratio between the minimum radius of the brane and the outer horizon radius becomes very large. We further remark (see Appendix C) that this non-extremal black hole solution is always dominant in the thermodynamic ensemble when $\tau_0 > 0$. This result was not feasible in the AdS-Schwarzschild case⁴ and is first main result of this work.

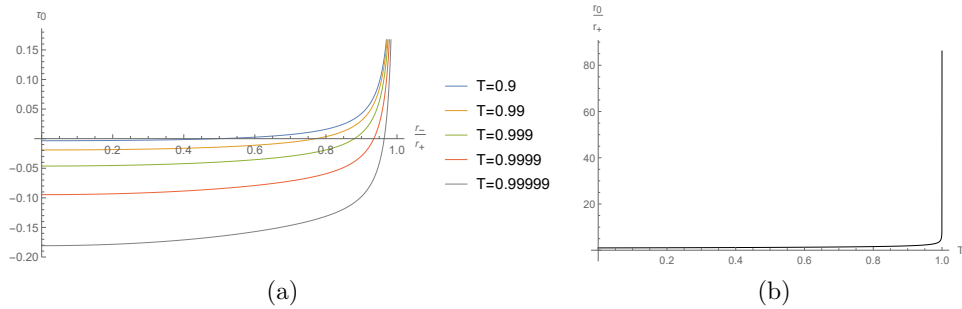


Figure 3: **Euclidean sensible solutions.** (a) The preparation time τ_0 is positive for every value of the tension T for a black hole sufficiently close to extremality. $d = 4$, $r_+ = 100$, $L_{AdS} = 1$. (b) The minimum radius of the brane r_0 grows with the tension T . $d = 4$, $r_+ = 100$, $r_- = 99.9$, $L_{AdS} = 1$.

3 Lorentzian analysis and braneworld cosmology

In order to study cosmological physics, we must find the Lorentzian geometry associated with the Euclidean picture outlined above. Consider the state (1), obtained taking the $\tau = 0, \pm\beta/2$ slice of the thermal circle (where the brane reaches its minimum radius r_0), and evolve it in Lorentzian time. The corresponding geometry is a maximally extended AdS-RN black hole with the ETW brane cutting off part of the left asymptotic region. The effect of the transition to Lorentzian time on equation (6) is to flip the sign of the radicand, thus the RHS is now real only if $r_0^- < r < r_0^+$. The minimum radius in Euclidean signature is a maximum radius in Lorentzian signature. Therefore the brane expands and contracts crossing the two horizons of the black hole, but, differently from the AdS-Schwarzschild case, it never reaches the singularity (see Figure 1).

Defining the brane proper time $d\lambda^2 = [f(r) - r'^2/f(r)]dt^2$, the metric induced on the brane takes the form

$$ds_{ETW}^2 = -d\lambda^2 + r^2(\lambda)d\Omega_{d-1}^2 \quad (7)$$

which is a closed FLRW metric where the brane radius $r(\lambda)$ plays the role of the scale factor, ranging between r_0^- and r_0^+ and satisfying the Friedmann equation

$$\left(\frac{\dot{r}}{r}\right)^2 = -\frac{1}{r^2} + \frac{2\mu}{r^d} - \frac{Q^2}{r^{2d-2}} + \left(T^2 - \frac{1}{L_{AdS}^2}\right) \quad (8)$$

where the dot indicates a derivative with respect to the proper time. For $d = 4$, this result (already obtained in refs.^{17,20}) shows that an observer comoving with the brane interprets the motion of the brane in the bulk as the expansion and contraction of a closed FLRW universe in the presence of radiation (with energy density proportional to the mass of the black hole), a negative cosmological constant $\Lambda_4 = 3(T^2 - 1/L_{AdS}^2)$ (which is very small when $T \rightarrow T_{crit}$) and stiff matter^{20,41} with negative energy density (proportional to the charge of the black hole).

From the bulk point of view, the existence of a minimum radius is due to the repulsive nature of the RN singularity, while from the braneworld point of view, the (repulsive) stiff matter term is responsible for the absence of the cosmological singularity, replaced by a Big Bounce.⁴¹ In principle, gluing together more patches of the AdS-RN bulk spacetime, we can obtain a cyclical cosmology. However, the instability of the Cauchy horizon against even small perturbations suggests that, in the region near the bounce, the present description of the brane evolution is not reliable.⁴² When the charge of the black hole vanishes, we recover the AdS-Schwarzschild description of a Big Bang-Big Crunch braneworld cosmology. We emphasize that the cosmological interpretation is not appropriate in the region where the Big Bounce takes place, because a 4-dimensional description of gravity localized on the brane is achievable only when the brane sits far from the black hole horizon.

4 Gravity localization

The remaining issue is whether observers on the brane see approximately four-dimensional gravity. Randall and Sundrum showed^{26,27} that a 4-dimensional Minkowski brane embedded in a warped AdS₅ spacetime supports a normalizable graviton zero-mode bound on the brane, reproducing 4-dimensional gravity. The bound mode is lost in the presence of an AdS-Schwarzschild black hole in the bulk,²⁹ but a resonant quasi-bound mode with a finite lifetime persists when the brane is static and far from the black hole horizon.³⁰ This is a metastable mode that, after a finite lifetime, “leaks” into the bulk and falls into the black hole horizon. The shorter the spatial scale of the gravitational perturbation, the longer it is bound on the brane. Gravity is therefore locally localized both in space and in time, meaning that it will look 4-dimensional to an observer living on the brane, but only on spatial and time scales smaller than the cosmological ones.

Clarkson and Seahra³⁰ focused their attention mainly on the small black hole case ($r_H < L_{AdS}$). Since sensible Euclidean solutions with $r_0/r_+ \gg 1$ are achievable only if the black hole is large, our generalization of their work to the AdS-RN spacetime is focused on the $r_+ \gg L_{AdS}$ case (see Appendix E).

Let us consider a linear perturbation of the metric $\delta g_{\mu\nu} = g_{\mu\nu} - g_{\mu\nu}^0$, $\mu, \nu = 0, \dots, d$. As a tensor on a spatial slice at constant radius ($t = const$, $r = const$), it can be decomposed into scalar, vector and tensor components.⁴³ The graviton mode of interest is the tensor component which has $\delta g_{t\mu} = \delta g_{r\mu} = 0$. We also use the transverse-traceless (TT) gauge condition $\delta g_{\mu}^{\mu} = 0 = \nabla^{\mu} \delta g_{\mu\nu}$. It is useful to introduce the d -dimensional coordinates and parameters $y = r/r_+$, $\tilde{t} = t/r_+$, $\gamma = L_{AdS}/r_+$, $q = Q/r_+^{d-2}$ and to decompose the metric perturbation in terms of tensor harmonics $\mathbb{T}_{ij}^{(k)}$ (with $i, j = 1, \dots, d-2$) on the unit $(d-1)$ -sphere. They satisfy $\Delta_{d-1} \mathbb{T}_{ij}^{(k)} = -k^2 \mathbb{T}_{ij}^{(k)}$, where Δ_{d-1} is the $(d-1)$ -dimensional covariant Laplacian on the unit $(d-1)$ -sphere and $k^2 = l(l+d-2) - 2$, with $l = 1, 2, \dots$ generalized angular momentum.

Defining the tortoise coordinate $dr^* = dy/f(y)$ and studying the problem in the frequency domain, the linearized Einstein equations can be recast in the form of a one-

dimensional Schrödinger equation for each tensor mode:

$$-\partial_{r^*}^2 \psi_{k,\omega}(r^*) + V_k[y(r^*)] \psi_{k,\omega}(r^*) = \omega^2 \psi_{k,\omega}(r^*) \quad (9)$$

where the potential reads:

$$V_k(y) = f(y) \left[\frac{d^2 - 1}{4\gamma^2} + \frac{d^2 - 4d + 11 + k^2}{4y^2} + \frac{(d-1)^2 \left(1 + \frac{1}{\gamma^2} + q^2\right)}{4y^d} - \frac{(d-1)(3d-5)q^2}{4y^{2d-2}} \right]. \quad (10)$$

This potential diverges for $r^* = r_\infty^*$ (where $y(r_\infty^*) = \infty$) and vanishes exponentially for $r^* \rightarrow -\infty$, at the black hole horizon.

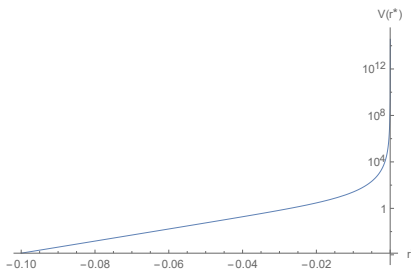


Figure 4: **Potential $V_k[y(r^*)]$ - Large black hole.** $r_+ = 100$, $r_- = 99.9$, $L_{AdS} = 1$. The potential diverges for $r_\infty^* = 4.94 \cdot 10^{-5}$ and vanishes exponentially at the horizon $r^* \rightarrow -\infty$.

Now we need to find a boundary condition on the ETW brane, which cuts off the radial coordinate at $r^* = r_b^* < r_\infty^*$. If the brane is moving in the bulk, this is a non-trivial task. We assume that the brane is moving adiabatically with respect to the time scale of the perturbation, and consider it effectively static at a position $r^* = r_b^*$, verifying later the reliability of the adiabatic approximation. Under this assumption, the linearized version of equation (5) provides the boundary condition $\partial_{r^*} \psi_{k,\omega}|_{r^*=r_b^*} = (d-1)f(y)/(2y) \cdot \psi_{k,\omega}|_{r^*=r_b^*}$, with $y = y(r^*)$. Requiring this boundary condition is equivalent to add to the potential (10) a negative delta at the position of the brane, whose depth is $(d-1)f(y)/y$. In the original Randall-Sundrum model, such a delta guarantees the existence of the zero bound mode. The rapid vanishing behaviour of the potential (10) at the black hole horizon implies that only a metastable, quasi-bound mode with complex frequency $\omega = \bar{\omega} + i\Gamma/2$ and pure infalling boundary condition at the black hole horizon (typical of quasi-normal modes) can be present in our setup. In the large black hole case ($\gamma \ll 1$) this is the only resonant mode.³⁰

Focusing on the $d = 4$, $\gamma \ll 1$ case of interest, we use the trapping coefficient method³⁰ to find the real and imaginary parts of the frequency of the quasi-bound mode. For a given value of the charge of the black hole, there are three control parameters: the size of the black hole γ , the position of the brane $r^*(y_b)$, and the angular momentum l . We find that, when the brane is sufficiently far from the horizon of the

black hole, $\bar{\omega} \gg \Gamma$ (i.e. the mode is long-lived) and the graviton is very well localized on the brane (see Figure 5). Such a localization is lost if the brane radius becomes too large. Increasing the size of the black hole, the brane must sit farther from the horizon to retain the long-lived quasi-bound mode. Gravity localization is also more efficient for higher values of the angular momentum l . Increasing l means probing shorter distances on the brane. Therefore, this result is in accordance with our expectation to obtain a 4-dimensional effective description of gravity only locally.

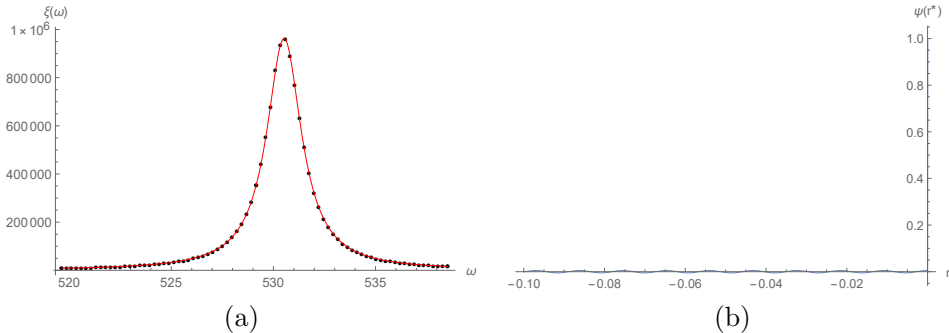


Figure 5: **Quasi-bound mode wavefunction.** $d = 4$, $r_+ = 100$, $r_- = 99.9$, $L_{AdS} = 1$, $l = 5$, $y_b = 34.62$. (a) Breit-Wigner peak of the squared trapping coefficient $\xi(\omega)$ at the frequency of the quasi-bound mode. The fit gives $\bar{\omega} = 583.6$, $\Gamma = 17.28$. (b) The quasi-bound mode wavefunction oscillates in the near-horizon region and grows very fast near $r_b^* = 4.65 \cdot 10^{-5}$, meaning that the mode is very well localized on the brane.

The last step is to verify that the adiabatic approximation is reasonable. One must compare the time scale of oscillation $t_o = 1/\bar{\omega}$ with the ‘‘Hubble time’’ $T_H = y(t)/y'(t)$, determined by the Lorentzian version of equation (6). The adiabatic approximation is reliable if $t_o \ll T_H$ and if the condition $(y')^2/f^2(y) \ll 1$ is satisfied. For given values of charge and tension, the approximation is arbitrarily good when approaching the inversion point in the trajectory of the brane, where y' vanishes. But it holds also for a significant portion of the trajectory of the brane, as quantified by the ratio between the proper time spent to cover the part of trajectory where the approximation is reliable and the total amount of proper time for the entire trajectory. As an example, for the set of parameters considered in Table 1, if we accept $t_o \sim T_H/10$ as the threshold for the validity of the adiabatic assumption, the latter holds for $\sim 55\%$ of the total amount of brane proper time. The decay time $t_d = 2/\Gamma$ is almost always considerably larger than the Hubble time, meaning that our analysis loses significance before the quasi-bound mode leaks into the bulk. We finally remark that the time of oscillation of the mode is very close to the one expected for a 4-dimensional metric perturbation of the Einstein-static universe $t_{GR} = y_b/\sqrt{f(y_b)(l+2)l}$. The local localization of gravity on the Euclidean-sensible braneworld solution is the second main result of this work.

y_b	T_H	t_o	t_d	$(y')^2 / [f(y)]^2$	$\lambda(y_b) / \lambda_{tot}$
30	$1.762 \cdot 10^{-3}$	$9.172 \cdot 10^{-4}$	0.08370	$3.581 \cdot 10^{-6}$	0.9764
45	$2.698 \cdot 10^{-3}$	$9.190 \cdot 10^{-4}$	0.1880	$6.786 \cdot 10^{-7}$	0.9465
60	$3.716 \cdot 10^{-3}$	$9.229 \cdot 10^{-4}$	0.3342	$2.012 \cdot 10^{-7}$	0.9035
75	$4.875 \cdot 10^{-3}$	$9.282 \cdot 10^{-4}$	0.5226	$7.484 \cdot 10^{-8}$	0.8459
90	$6.282 \cdot 10^{-3}$	$9.350 \cdot 10^{-4}$	0.7516	$3.129 \cdot 10^{-8}$	0.7713
105	$8.178 \cdot 10^{-3}$	$9.432 \cdot 10^{-4}$	1.026	$1.356 \cdot 10^{-8}$	0.6748
120	0.01124	$9.530 \cdot 10^{-4}$	1.339	$5.495 \cdot 10^{-9}$	0.5462
135	0.01895	$9.645 \cdot 10^{-4}$	1.713	$1.527 \cdot 10^{-9}$	0.3540
145.1 (max)	∞	$9.733 \cdot 10^{-4}$	1.956	0	0

Table 1: **Adiabatic approximation.** Time scales of oscillation, decay and motion of the brane, ratio $(y')^2 / [f(y)]^2$ and fraction of proper time left between y_b and y_b^{max} . The chosen parameters are: $\gamma = 0.01$, $L_{AdS} = 1$, $r_+ = 100$, $r_- = 99.9$, $l = 10$, $T = 0.999999999$. The position accompanied by “max” is the maximum position reached by the brane for the chosen parameters. The Euclidean solution corresponding to this choice of parameters is sensible and dominant in the thermodynamic ensemble.

5 Discussion

In this work we proved that it is possible to build a holographic braneworld cosmology model which admits locally a 4-dimensional effective description of gravity. An interesting open question is if this framework can be extended to different cosmological models, eventually including a de Sitter phase that could match our current observational data, and if gravity localization is achievable on even larger scales in such setups. Understanding gravity localization beyond the adiabatic approximation would also be interesting.

The holographic dual description presents many non-trivial issues to be explored. Determining which CFT observables are able to probe the physics behind the horizon of the black hole, and therefore the braneworld cosmology, is crucial. If the brane is not too far from the black hole horizon, one possibility is the entanglement entropy of large spatial regions of the CFT,^{4,44,45} while additional information can be extracted from the holographic complexity, even if its CFT interpretation is not completely clear yet. It is also important to identify field theories with the right boundary states to make our construction work and verify the stability of the solutions in the full theory. For example, one should check that scalar fields do not condense in the near-extremal black hole background (or that the desired properties persist in such a condensed state). Given such a theory, it should be possible to simulate it on a quantum computer,^{8,46–48} thereby opening up the possibility to experimentally study holographic braneworld cosmology.

Although many questions still need to be answered, the model presented in this paper shows the possibility to holographically describe a FLRW cosmology using AdS/CFT, bringing us one step closer to the understanding of quantum gravity in a cosmological universe.

Acknowledgements

This work was supported in part by the U.S. Department of Energy, Office of Science, Office of High Energy Physics QuantISED Award DE-SC0019380 and by the Simons Foundation via the It From Qubit collaboration. We thank M. Van Raamsdonk, C. Waddell, D. Wakeham, M. Rozali, S. Cooper, R. Sundrum, R. Bousso, and J. Maldacena for useful discussions.

Appendices

A Euclidean action and Einstein-Maxwell equations

The total Euclidean action for the bulk spacetime is given by

$$I_{bulk} = -\frac{1}{16\pi G} \int_{\mathcal{M}} d^{d+1}x \sqrt{g} (R - 2\Lambda - 4\pi G F_{\mu\nu} F^{\mu\nu}) + I_{GHY} + I_{bound}^{em} \quad (11)$$

where \mathcal{M} is the $(d+1)$ -dimensional spacetime manifold, g is the determinant of the bulk metric, R is the Ricci scalar, $\Lambda = -d(d-1)/(2L_{AdS}^2)$ is the cosmological constant, I_{GHY} is the Gibbons-Hawking-York term for the asymptotic boundary and

$$I_{bound}^{em} = - \int_{\partial\mathcal{M}_\infty} d^d x \sqrt{\gamma} F^{\mu\nu} n_\mu A_\nu \quad (12)$$

with γ determinant of the metric induced on the asymptotic boundary $\partial\mathcal{M}_\infty$ and n_μ dual vector normal to the boundary. The term I_{bound}^{em} is needed³⁸⁻⁴⁰ because we keep the charge fixed instead of the potential when we vary the action (11). This choice is preferable since we are interested in controlling the charge in order to approach the extremal black hole case and obtain a sensible Euclidean solution for a near-critical brane. The electromagnetic four-potential $A_\mu = (A_t, \vec{0})$ for a point charge in the origin reads:

$$A_t = \sqrt{\frac{d-1}{8\pi G(d-2)}} \left(\frac{Q}{r^{d-2}} - \frac{Q}{r_+^{d-2}} \right) \quad (13)$$

where we chose the outer (event) horizon of the black hole $r = r_+$ to be the zero-potential surface and Q is the charge parameter of the black hole, related to the point charge \tilde{Q} (charge of the black hole) by^{31,39,40}

$$Q = \sqrt{\frac{8\pi G}{(d-1)(d-2)}} \frac{\tilde{Q}}{V_{d-1}} \quad (14)$$

with V_{d-1} volume of the $(d-1)$ -dimensional unit sphere. The electromagnetic tensor is standardly defined as $F_{\mu\nu} = \partial_\mu A_\nu - \partial_\nu A_\mu$. The action for the End-of-the-World brane is reported in equation (2), where I_{ETW}^{em} has the same form (12) of the electromagnetic

boundary term for the asymptotic boundary, with $\gamma \rightarrow h$ and n_μ dual vector normal to the ETW brane. The extrinsic curvature appearing there is defined as

$$K_{ab} = \nabla_\mu n_\nu e_a^\mu e_b^\nu, \quad e_a^\mu = \frac{dx^\mu}{dy^a}. \quad (15)$$

A variation of the total action for the bulk and the brane leads to a set of three equations: equation (5) (describing the motion of the brane in the bulk spacetime), the Einstein-Maxwell equations for the bulk

$$R_{\mu\nu} - \frac{1}{2}g_{\mu\nu}(R - 2\Lambda) = 8\pi GT_{\mu\nu}^{bulk} \quad (16)$$

with $R_{\mu\nu}$ Ricci tensor, and the Maxwell equation

$$\nabla_\mu (\sqrt{-g}F^{\mu\nu}) = 0. \quad (17)$$

The bulk stress-energy tensor appearing in equation (16) is the electromagnetic stress-energy tensor:

$$T_{\mu\nu}^{bulk} = g^{\rho\sigma} F_{\mu\rho} F_{\nu\sigma} - \frac{1}{4}g_{\mu\nu} F_{\rho\sigma} F^{\rho\sigma}. \quad (18)$$

The static and spherically symmetric metric reported in equation (3) is a solution of the Einstein-Maxwell equations (16) and the mass parameter μ appearing in equation (4) (which is valid only for $d > 2$) is related to the ADM mass of the black hole by

$$\mu = \frac{8\pi GM}{(d-1)V_{d-1}}. \quad (19)$$

In order to approach, in our numerical analysis, the extremal black hole case for a fixed event horizon size by controlling the Cauchy horizon radius it is useful to express the mass and the charge parameters in terms of r_+ and r_- :

$$\mu = \frac{L_{AdS}^2 \left[r_+^{2(d-2)} - r_-^{2(d-2)} \right] + r_+^{2d-2} - r_-^{2d-2}}{2L_{AdS}^2 (r_+^{d-2} - r_-^{d-2})}; \quad (20)$$

$$Q^2 = r_+^{d-2} r_-^{d-2} \left[\frac{L_{AdS}^2 (r_+^{d-2} - r_-^{d-2}) + r_+^d - r_-^d}{L_{AdS}^2 (r_+^{d-2} - r_-^{d-2})} \right]. \quad (21)$$

It is also convenient to eliminate the mass parameter from the expression of the $\tau\tau$ component of the metric $f(r)$:

$$f(r) = 1 + \frac{r^2}{L_{AdS}^2} - \frac{r_+^{d-2}}{r^{d-2}} \left(1 + \frac{r_+^2}{L_{AdS}^2} \right) + \frac{Q^2}{r^{d-2}} \left(\frac{1}{r^{d-2}} - \frac{1}{r_+^{d-2}} \right) \quad (22)$$

which can be rewritten, using the adimensional coordinates introduced in Section 4, in a form more functional for the gravity localization analysis

$$f(y) = \frac{[y^4 + (\gamma^2 + 1)y^2 - \gamma^2 q^2](y^2 - 1)}{\gamma^2 y^4}. \quad (23)$$

For completeness, we report here also the form of the $\tau\tau$ component of the metric for the BTZ charged black hole (i.e. for $d = 2$) as a function of the ADM mass M and the charge of the black hole \tilde{Q} , in units such that $G_3 = 1/8$:³⁴

$$f(r) = \frac{r^2}{L_{AdS}^2} - M - \tilde{Q}^2 \ln\left(\frac{r}{L_{AdS}}\right). \quad (24)$$

Finally, the Ricci scalar for a spherically symmetric metric of the form (3) takes in general the form

$$R = -\frac{r^2 f''(r) + 2r(d-1)f'(r) + (d-1)(d-2)f(r) - (d-1)(d-2)}{r^2}. \quad (25)$$

Substituting equation (4), we obtain, for $d > 2$

$$R = -\frac{d(d+1)}{L_{AdS}^2} - \frac{(d-3)(d-2)Q^2}{r^{2d-2}}. \quad (26)$$

B Euclidean analysis - details

In order to avoid a conical singularity, the Euclidean time τ must be periodic with periodicity given by

$$\beta = \frac{2\pi}{k_g}. \quad (27)$$

k_g is the surface gravity, which for the static and spherically symmetric black holes reads

$$k_g = \frac{f'(r)}{2} \Big|_{r=r_H} \quad (28)$$

where r_H is the event horizon radius. For a Reissner-Nordström black hole $r_H = r_+$. Using equation (22), for $d > 2$ we find the Euclidean periodicity

$$\beta = \frac{4\pi L_{AdS}^2 r_+^{2d-3}}{(d-2)L_{AdS}^2 \left[r_+^{2(d-2)} - Q^2 \right] + dr_+^{2d-2}}. \quad (29)$$

The spherically symmetric ETW brane can be parameterize with $r = r(\tau)$. Analogously to the AdS-Schwarzschild case,⁴ the one-form dual to the unit vector normal to the brane is given by

$$n_\mu = \gamma(-r', 1, 0, 0), \quad \gamma = \sqrt{\frac{f(r)}{f^2(r) + (r')^2}} \quad (30)$$

with $r' = dr/d\tau$. The metric induced on the brane reads

$$\begin{aligned} h_{\tau\tau} &= f(r) + \frac{(r')^2}{f(r)}; \\ h_{\phi_i\phi_i} &= g_{\phi_i\phi_i} \quad i = 1, \dots, d-1 \end{aligned} \quad (31)$$

where ϕ_i are the coordinates on the sphere directions. Using the definition of the extrinsic curvature (15) and equation (30), the $\tau\tau$ component of equation (5) leads to equation (6), that we report here:

$$\frac{dr}{d\tau} = \pm \frac{f(r)}{Tr} \sqrt{f(r) - T^2 r^2}. \quad (32)$$

The + (−) sign corresponds to the contracting (expanding) phase. Indeed, as it is clear from Figure 2, during the contraction the Euclidean time decreases (clockwise) from $\tau = -\tau_0$ to $\tau = -\beta/2$, therefore the $dr/d\tau > 0$; during the expansion the time decreases from $\tau = \beta/2$ to $\tau = \tau_0$, and $dr/d\tau < 0$. It is easy to show that, if equation (32) is satisfied, the other components of equation (5) are identically fulfilled.

The minimum radius r_0 is defined by the largest zero of the RHS of equation (32), as discussed in Section 2. For a vanishing tension, clearly $r_0 = r_+$, since $f(r_+) = 0$ by definition of horizon. It is not difficult to show that for $d > 2$ and a critical brane, i.e. for $T = T_{crit} = 1/L_{AdS}$, the equation $f(r) = T^2 r^2$ can be solved analytically, leading to two solutions $r_0^+ > r_+$ and $r_0^- < r_-$, and therefore $r_0 = r_0^+ > r_+$. A numerical evaluation shows that for $0 < T < T_{crit}$ the latter property still holds. The ratio r_0/r_+ increases when the tension increases. In particular, if the black hole is big (meaning $r_+ \gg L_{AdS}$), it is possible to obtain a very large ratio r_0/r_+ by approaching the critical value of the tension (see Figure 3(b)). If the black hole is small, the ratio is never large, preventing, as we observed, gravity localization on the brane.

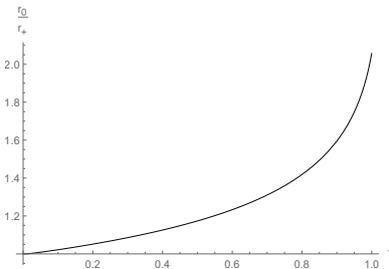


Figure 6: **Minimum brane radius - Small black hole.** The minimum radius of the brane r_0 grows with the tension T , but it never becomes much larger than the black hole horizon. $d = 4$, $r_+ = 1$, $r_- = 0.99$, $L_{AdS} = 1$.

Since we are interested in time-symmetric solutions, we can require the brane to reach its minimum radius for $\tau = \pm\beta/2$, defining $r_0 = r(\tau = \pm\beta/2)$. Up to a constant $\beta/2$ (which cancels out when adding up the Euclidean times necessary for the expanding

and the contracting phases), the brane locus is given by

$$\tau(r) = \int_{r_0}^r d\hat{r} \frac{T\hat{r}}{f(\hat{r})\sqrt{f(\hat{r}) - T^2\hat{r}^2}}. \quad (33)$$

The total Euclidean time necessary for the brane to go from $r = r_0$ to $r = \infty$, i.e. to cover half of its trajectory, is

$$\Delta\tau = \int_{r_0}^{\infty} dr \frac{Tr}{f(r)\sqrt{f(r) - T^2r^2}}. \quad (34)$$

The Euclidean preparation time τ_0 is given by the residual Euclidean periodicity:

$$\tau_0 = \frac{\beta - 2\Delta\tau}{2} = \frac{2\pi L_{AdS}^2 r_+^{2d-3}}{(d-2)L_{AdS}^2 (r_+^{2(d-2)} - Q^2) + dr_+^{2d-2}} - \Delta\tau. \quad (35)$$

For a critical brane we obtain:

$$\Delta\tau_{crit} = \frac{1}{L_{AdS}} \int_{r_0}^{\infty} dr \frac{r}{\left(1 + \frac{r^2}{L_{AdS}^2} - \frac{2\mu}{r^{d-2}} + \frac{Q^2}{r^{2(d-2)}}\right) \sqrt{1 - \frac{2\mu}{r^{d-2}} + \frac{Q^2}{r^{2(d-2)}}}} \quad (36)$$

and this expression is logarithmically divergent at infinity. For $T > T_{crit}$, the square root $\sqrt{f(r) - T^2r^2}$ becomes imaginary for large values of r . Thus, $\Delta\tau$, and therefore the preparation time τ_0 , are well defined only for $T < T_{crit}$.

Our numerical evaluation shows that, given a value for the outer horizon radius r_+ and for the brane tension $T < T_{crit}$, it is always possible to obtain a positive preparation time (i.e. a sensible Euclidean solution, and a dual description in terms of an Euclidean-time-evolved charged boundary state of a CFT living on the boundary of the right asymptotic region of the black hole) by increasing the size of the inner horizon radius r_- , which means by increasing the charge of the black hole. For $T \rightarrow T_{crit}$, we need $r_- \rightarrow r_+$ in order to retain a sensible Euclidean solution, i.e. the black hole must approach extremality. This feature guarantees that, for a large black hole sufficiently close to extremality, we can find a sensible Euclidean solution with the minimum radius of the brane (which is the maximum radius in Lorentzian signature) consistently larger than the black hole event horizon. As we have pointed out, this is a necessary condition in order to achieve gravity localization on the brane. In the AdS-Schwarzschild case, which is the $Q \rightarrow 0$ limit of our analysis, this result is clearly impossible to obtain. Therefore, for an uncharged black hole gravity localization and positive preparation time mutually exclude each other, and a holographic braneworld cosmology picture is not feasible.⁴

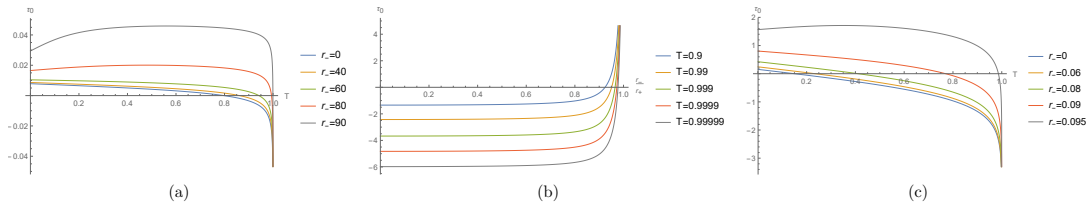


Figure 7: **Preparation time.** (a) Large black hole case. Approaching the extremal black hole, τ_0 is positive for a larger range of values for the tension T . $d = 4$, $r_+ = 100$, $L_{AdS} = 1$. (b)-(c) Small black hole case. The behaviour is similar to the large black hole case (the analogous of (b) is reported in Figure 3(a)). $d = 4$, $r_+ = 0.1$, $L_{AdS} = 1$.

C Action comparison

In order to understand if the non-extremal AdS-RN solution we studied is dominant in the Euclidean path integral, we must compare its on-shell action with other possible phases contributing to the path integral. The dominant phase will be the one with smallest action. As we have already pointed out, we will focus our attention on the fixed charge case. This choice corresponds to a canonical ensemble, where the temperature and the charge are held fixed. Note that this implies that (differently from the fixed potential case) the variation of the potential does not vanish on the boundary. For this reason, we need to add the electromagnetic boundary terms (12) for the asymptotic boundary and the brane to the action. For fixed charge, the other possible phase is represented by the extremal AdS-RN black hole with the same charge as the corresponding non-extremal solution (for a complete treatment of the AdS-RN phase structure for fixed charge and fixed potential without the ETW brane see refs.^{39,40}). The CFT state corresponding to the fixed charge ensemble is the Euclidean-time-evolved boundary state with fixed charge reported in equation (1). It is clear that the two Euclidean solutions contributing to the gravity path integral dual to the state (1) must have the same charge and the same preparation time τ_0 . We will use this property in order to match the two geometries in the asymptotic region, procedure needed in order to regularize the Euclidean action and compare the two actions.^{4,39,40} We will now briefly review some useful properties of the extremal AdS-RN black hole.

Extremal AdS-RN black hole

For the extremal AdS-Reissner-Nordström black hole, the two solutions r_+ and r_- of $f_e(r) = 0$ coincide, defining the extremal horizon radius r_e . Therefore, also the relationship $f'_e(r)|_{r=r_e} = 0$ must hold. By requiring the two conditions to be satisfied, we obtain

for the extremal mass and charge parameters:

$$2\mu_e = 2r_e^{d-2} + \frac{2d-2}{d-2} \frac{r_e^d}{L_{AdS}^2}; \quad (37)$$

$$Q_e^2 = r_e^{2d-4} + \frac{d}{d-2} \frac{r_e^{2d-2}}{L_{AdS}^2}. \quad (38)$$

We remark how, by fixing the charge of the black hole, the extremal horizon radius is uniquely determined.

Another important feature of the extremal black hole is that, since $f'_e(r)|_{r=r_e} = 0$, the Euclidean periodicity (27) diverges, i.e. the temperature of the extremal black hole vanishes. Nonetheless, it has been demonstrated^{36,39,40} that an arbitrary Euclidean periodicity can be chosen for the extremal RN black hole without running into a conical singularity. Physically, this means that an extremal RN black hole can be in thermodynamic equilibrium with a thermal bath at an arbitrary temperature. In the following we will use this feature, fixing a total Euclidean periodicity β_e for the extremal black hole that will be determined by matching the geometries of the non-extremal and the extremal black holes in the asymptotic regions. Given β_e , the extremal horizon radius r_e and the expression (38) for the extremal charge, the same Euclidean analysis carried out in Section A can be applied to the extremal case.

Before explicitly evaluating the difference of the two Euclidean actions for the non-extremal and extremal black holes, one more remark is needed. In general, the phase structure is more complicated than the one we are going to study. In particular, for a given small charge $Q < Q_{crit}$ and some range of temperatures, three different non-extremal black holes with the same temperature but different horizon radius can exist.³⁹ Indeed, for $Q < Q_{crit}$, there exist turning points for the Euclidean periodicity β as a function of the external horizon r_+ , which disappear for $Q > Q_{crit}$. The critical charge can be obtained from the condition $\partial_{r_+}\beta = 0 = \partial_{r_+}^2\beta$, and reads:³⁹

$$Q_{crit}^2 = \frac{1}{(d-1)(2d-3)} \left[\frac{(d-2)^2}{d(d-1)} \right] L_{AdS}^{2d-4}. \quad (39)$$

The coexistence of different non-extremal black holes implies the necessity of studying which one of them has the smallest action, before a comparison with the extremal case can be made. To do so, we should fix an Euclidean periodicity β and a charge Q , find the different corresponding values of r_+ and compare the actions for each of them.

Nonetheless, since, as we have already pointed out, we are interested in solutions involving near-critical branes, and this requires to have a black hole near extremality in order to have a positive preparation time, we are safely into the region where only one non-extremal phase exists.³⁹ Therefore, we are allowed to choose r_+ and r_- (and therefore the charge) independently, and compare directly the resulting action with the corresponding extremal action with the same charge.

Bulk action

Let us evaluate the three terms of the bulk action (11) separately in the non-extremal case. First, using equation (13), the only non vanishing components of the electromagnetic tensor are $F_{\tau r} = -F_{r\tau}$, and we obtain

$$F_{\mu\nu}F^{\mu\nu} = -\frac{(d-1)(d-2)}{4\pi G} \frac{Q^2}{r^{2d-2}}. \quad (40)$$

Using equation (25) for the Ricci scalar, the relationship between Λ and L_{AdS} , and noting that $\sqrt{g} = r^{d-1}$, the first term of the bulk action reads

$$I_{bulk}^{(1)} = \frac{dV_{d-1}}{8\pi GL_{AdS}^2} \int dr d\tau r^{d-1} - \frac{(d-2)V_{d-1}Q^2}{8\pi G} \int dr d\tau \frac{1}{r^{d-1}}. \quad (41)$$

Recalling that part of the Euclidean geometry is cut off by the ETW brane parameterized by $\tau(r)$, we can rewrite this integral as the integral in the entire spacetime minus the excised part. In order to avoid divergences, we must also introduce a cut-off R in the asymptotic region. After a few steps, the result turns out to be

$$\begin{aligned} I_{bulk}^{(1)} = & \frac{V_{d-1}}{8\pi GL_{AdS}^2} \left[\beta(R^d - r_+^d) - 2(r^d \tau(r)) \Big|_{r_0}^R + 2 \int_{r_0}^R dr r^d \frac{\partial \tau}{\partial r} \right] \\ & + \frac{V_{d-1}Q^2}{8\pi G} \left[\beta \left(\frac{1}{R^{d-2}} - \frac{1}{r_+^{d-2}} \right) - 2 \left(\frac{\tau(r)}{r^{d-2}} \right) \Big|_{r_0}^R + 2 \int_{r_0}^R dr \frac{1}{r^{d-2}} \frac{\partial \tau}{\partial r} \right] \end{aligned} \quad (42)$$

where β is given by equation (29).

The Gibbons-Hawking-York term I_{GHY} gives a vanishing contribution to the action difference for asymptotically AdS spacetimes^{39,40,49} and therefore we can neglect it. The electromagnetic boundary term finally reads

$$I_{bound}^{em} = -\frac{(d-1)V_{d-1}Q^2\tau_0}{4\pi G} \left(\frac{1}{R^{d-2}} - \frac{1}{r_+^{d-2}} \right). \quad (43)$$

Brane action

Tracing equation (5) we obtain

$$K - (d-1)T = T. \quad (44)$$

Parameterizing again the brane with $\tau(r)$, and using equation (32), the determinant of the metric induced on the brane reads:

$$\sqrt{h} = \pm \frac{1}{T} f(r) r^{d-2} \frac{\partial \tau}{\partial r} \quad (45)$$

where the + (−) sign is for the contracting (expanding) phase. Considering the contributions of both these two phases and using the expression (30) for the dual vector normal to the brane, the total action for the ETW brane reads

$$\begin{aligned}
 I_{ETW} = & -\frac{V_{d-1}}{4\pi G} \int_{r_0}^R dr f(r) r^{d-2} \frac{\partial \tau}{\partial r} \\
 & + \frac{(d-1)V_{d-1}Q^2}{4\pi G r_+^{d-2}} \tau(r) \Big|_{r_0}^R - \frac{(d-1)V_{d-1}Q^2}{4\pi G} \int_{r_0}^R dr \frac{1}{r^{d-2}} \frac{d\tau}{dr}.
 \end{aligned} \tag{46}$$

Action difference

Using the definition (33), we note that $\tau(r_0) = 0$. Additionally, $\lim_{R \rightarrow \infty} \tau(R) = \Delta\tau$ and $\beta - 2\Delta\tau = 2\tau_0$. Since, after subtracting the extremal action from the non-extremal one, we will take the limit $R \rightarrow \infty$, for simplicity of notation we will substitute now $\tau(R) \rightarrow \Delta\tau$ and $\beta - 2\tau(R) \rightarrow 2\tau_0$, even if the limit has not been taken yet. Using the above cited relationships, the total action for the non-extremal black hole can be cast in the form

$$\begin{aligned}
 I_{tot} = & \frac{V_{d-1}}{8\pi G L_{AdS}^2} \left\{ 2\tau_0 R^d - \beta r_+^d - \frac{2(d-2)L_{AdS}^2 Q^2}{R^{d-2}} \tau_0 + \frac{(d-2)L_{AdS}^2 Q^2}{r_+^{d-2}} \beta \right. \\
 & \left. + 2 \int_{r_0}^R dr \left[\left(r^d - \frac{(d-2)L_{AdS}^2 Q^2}{r^{d-2}} - L_{AdS}^2 r^{d-2} f(r) \right) \frac{\partial \tau}{\partial r} \right] \right\}.
 \end{aligned} \tag{47}$$

We must now subtract from this action the equivalent action for the extremal black hole after matching the geometries in the asymptotic region, and then take the limit $R \rightarrow \infty$. The total action for the extremal black hole is given by equation (47) where all the quantities are substituted by their extremal counterparts ($r_+ \rightarrow r_e$, $\tau_0 \rightarrow \tau_0^e$, $\beta \rightarrow \beta_e$, $r_0 \rightarrow r_0^e$, $f(r) \rightarrow f_e(r)$, $Q \rightarrow Q_e$). As we have already mentioned, the Euclidean analysis carried out for the non extremal black hole is still valid by substituting $r_+ \rightarrow r_e$, and the total Euclidean periodicity β_e can be chosen arbitrarily.³⁶ Since we are interested in the fixed charge case, we can choose a charge, which will be the same for both the black holes ($Q = Q_e$), using equation (21) and selecting values for the outer and inner horizon radii (r_+ and r_-) of the non-extremal black hole. The extremal horizon radius r_e is then uniquely determined by equation (38). Therefore r_e can be written as a function of r_+ and r_- only. We will use this feature in our numerical analysis.

The choice of the (arbitrary) Euclidean periodicity for the extremal black hole is determined by the matching of the two geometries in the asymptotic region. In particular, we must match the proper Euclidean preparation times in the asymptotic region (i.e. for $r = R$):

$$2\tau_0 \sqrt{f(R)} = 2\tau_0^e \sqrt{f_e(R)}. \tag{48}$$

At lowest order in $1/R$, equation (48) gives

$$\tau_0^e \sim \tau_0(1 + A) \tag{49}$$

where, we have defined:

$$A = \frac{L_{AdS}^2}{R^d}(\mu_e - \mu) = \frac{L_{AdS}^2}{R^d} \left(r_e^{d-2} + \frac{d-1}{d-2} \frac{r_e^d}{L_{AdS}^2} - \frac{r_+^{d-2}}{2} - \frac{r_+^d}{2L_{AdS}^2} - \frac{Q^2}{2r_+^{d-2}} \right). \quad (50)$$

We emphasize that, at the asymptotic boundary (i.e. for $R \rightarrow \infty$), $\tau_0^e = \tau_0$, as we expect for two geometries dual to the state (1). The total Euclidean periodicity for the extremal black hole can then be set to be

$$\beta_e = 2\tau_0^e + 2\Delta\tau_e = 2\tau_0(1 + A) + 2\Delta\tau_e \quad (51)$$

where $\Delta\tau_e$ is defined in perfect analogy with the non-extremal case. Using equation (51) and the matching condition (49) and taking the limit $R \rightarrow \infty$, after some manipulation the difference between the non-extremal and the extremal action finally takes the form

$$\begin{aligned} \Delta I \equiv & \frac{8\pi GL_{AdS}^2}{V_{d-1}} \lim_{R \rightarrow \infty} (I - I_{ext}) = \\ & - \frac{2r_e^d \tau_0}{d-2} - 2L_{AdS}^2 r_e^{d-2} \tau_0 + L_{AdS}^2 r_+^{d-2} \tau_0 + r_+^d \tau_0 - \beta r_+^d + \frac{L_{AdS}^2 Q^2 \tau_0}{r_+^{d-2}} \\ & + 2r_e^d \Delta\tau_e + \frac{(d-2)L_{AdS}^2 Q^2 \beta}{r_+^{d-2}} - \frac{2(d-2)L_{AdS}^2 Q^2 \tau_0}{r_e^{d-2}} - \frac{2(d-2)L_{AdS}^2 Q^2 \Delta\tau_e}{r_e^{d-2}} \\ & - 2L_{AdS}^2 \int_{r_0^e}^{r_0} dr \left\{ \left[-r^{d-2} + r_e^{d-2} \left(1 + \frac{r_e^2}{L_{AdS}^2} \right) + \frac{Q^2}{r_e^{d-2}} - \frac{(d-1)Q^2}{r^{d-2}} \right] \frac{Tr}{f_e(r)\sqrt{f_e(r) - T^2 r^2}} \right\} \\ & + 2L_{AdS}^2 \int_{r_0}^{\infty} dr \left\{ \left[-r^{d-2} + r_+^{d-2} \left(1 + \frac{r_+^2}{L_{AdS}^2} \right) + \frac{Q^2}{r_+^{d-2}} - \frac{(d-1)Q^2}{r^{d-2}} \right] \frac{Tr}{f(r)\sqrt{f(r) - T^2 r^2}} \right. \\ & \left. - \left[-r^{d-2} + r_e^{d-2} \left(1 + \frac{r_e^2}{L_{AdS}^2} \right) + \frac{Q^2}{r_e^{d-2}} - \frac{(d-1)Q^2}{r^{d-2}} \right] \frac{Tr}{f_e(r)\sqrt{f_e(r) - T^2 r^2}} \right\}. \end{aligned} \quad (52)$$

When such a difference is negative, the non-extremal black hole phase has smaller action and is therefore dominant in the ensemble.

A numerical evaluation shows that, for $d = 4$ and for a range of parameters such that the Euclidean solution for the non-extremal black hole is sensible (i.e. $\tau_0 > 0$), ΔI is always negative. Therefore, differently from the AdS-Schwarzschild case,⁴ when the non-extremal AdS-RN solution admits a dual CFT description, it is also always dominant in the gravity path integral.

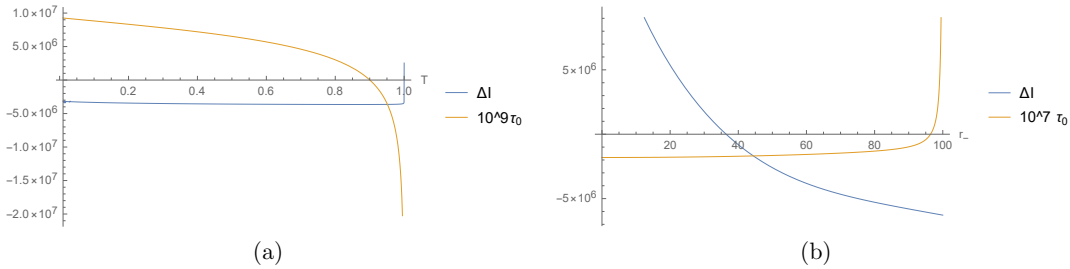


Figure 8: **Action difference - Large black hole.** (a) When the tension T is not too close to its critical value, $\tau_0 > 0$ and the non-extremal solution is always dominant. $d = 4$, $r_+ = 100$, $r_- = 50$, $L_{AdS} = 1$. (b) When the black hole is sufficiently close to extremality, $\tau_0 > 0$ and the Euclidean solution is sensible. The non-extremal solution is already dominant in the ensemble well before it happens. $d = 4$, $r_+ = 100$, $T = 0.99999$, $L_{AdS} = 1$. The same properties hold also for the small black hole case.

D Lorentzian analysis and braneworld cosmology - details

The initial condition for the Lorentzian time evolution is given by the $\tau = 0, \pm\beta/2$ slice of the Euclidean geometry, where the brane reaches its minimum radius r_0 . The time coordinate is analytically continued $\tau \rightarrow -it$, with t Lorentzian time. Further time evolution will be in Lorentzian signature. The brane locus is then given by

$$t(r) = \int_{r_0}^r d\hat{r} \frac{T\hat{r}}{f(\hat{r})\sqrt{T^2\hat{r}^2 - f(\hat{r})}}. \quad (53)$$

We explained that, in the Lorentzian case, the range of the radial coordinate is $r_0^- < r_0 < r_0^+ \equiv r_0$. Let us now focus on the Friedmann equation (considered in equation (8)) describing the evolution of the brane in terms of its proper time λ . By defining $L(r) = \ln r$ and $L_+ = L(r_+)$, it can be rewritten as

$$\dot{L}^2 + V(L) = T^2 \quad (54)$$

where

$$V[L(r)] = \frac{f(r)}{r^2}. \quad (55)$$

In this new coordinate, the motion of the brane can be regarded as the one of a particle with energy T^2 in the presence of a potential $V(L)$. The potential (55) naturally vanishes for $r = r_+$ and $r = r_-$. It has a local maximum and a local minimum in r_M and r_m respectively. For the local minimum $r_- < r_m < r_+$ and $V[L(r_m)] < 0$, while for the local maximum $r_M > r_+$ and $V[L(r_M)] > 1/L_{AdS}^2 = T_{crit}^2$. Additionally $\lim_{r \rightarrow \infty} V[L(r)] = T_{crit}^2$, while $\lim_{r \rightarrow 0} V[L(r)] = \infty$. The latter behaviour confirms that the brane radius cannot vanish, i.e. the brane undergoes a bounce for a minimum radius r_0^- . Differently from the small black hole case ($r_+ \lesssim L_{AdS}$), in the large black hole case ($r_+ \gg L_{AdS}$) the minimum of the potential is $V[L(r_m)] \sim 0$ and its local maximum is $V[L(r_M)] \sim T_{crit}^2$,

the latter meaning that the value of the potential at the peak is almost indistinguishable from its asymptotic value. As an example we report in Figure 9 a plot of the potential $V[L(r)]$ as a function of the radius of the brane r in the small and in the large black hole cases.

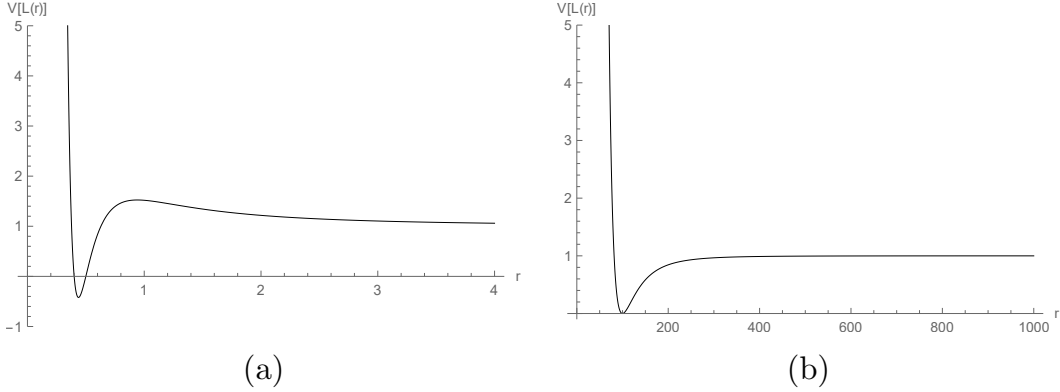


Figure 9: **Potential $V[\mathbf{L}(\mathbf{r})]$.** (a) Small black hole case. The peak at $r = r_M$ is particularly evident. $d = 4$, $r_+ = 0.5$, $r_- = 0.4$, $L_{AdS} = 1$. (b) Large black hole case. r_M is very large and the value of the potential at the peak is almost indistinguishable from the asymptotic value. $d = 4$, $r_+ = 100$, $r_- = 99.9$, $L_{AdS} = 1$.

The brane trajectory will be determined by the value of its tension (i.e. the energy of the particle). In particular, analogously to the AdS-Schwarzschild case,⁴ we can distinguish in general five different cases:

1. $\mathbf{T}^2 > \mathbf{V}[\mathbf{L}(\mathbf{r}_M)]$. The equation $f(r_0) = T^2 r_0^2$ has only one positive solution (r_0^-), which is by definition the position of the brane at $\lambda = 0$. Therefore, the brane radius decreases from $r = \infty$ to $r = r_0^-$ for negative time and then increases monotonically from $r = r_0^-$ to $r = \infty$ for positive time.
2. $\mathbf{T}^2 = \mathbf{V}[\mathbf{L}(\mathbf{r}_M)]$. The brane has constant radius $r = r_M$. This corresponds to an Einstein static universe.
3. $\mathbf{T}_{\text{crit}}^2 < \mathbf{T}^2 < \mathbf{V}[\mathbf{L}(\mathbf{r}_M)]$ - **Large \mathbf{r} branch.** The equation $f(r_0) = T^2 r_0^2$ admits three solutions. In particular, if we order such solutions as $r_0^{(3)} > r_0^{(2)} > r_0^{(1)}$, the quantity $\sqrt{T^2 r^2 - f(r)}$ is real for $r > r_0^{(3)}$ and for $r_0^{(1)} < r < r_0^{(2)}$. Thus, for large r , the behaviour is similar to the first case, with the brane trajectory starting from $r = \infty$, shrinking to $r = r_0^{(3)}$ for $\lambda = 0$ and expanding again to $r = \infty$.
4. $\mathbf{T}_{\text{crit}}^2 < \mathbf{T}^2 < \mathbf{V}[\mathbf{L}(\mathbf{r}_M)]$ - **Small \mathbf{r} branch.** This is the same situation as in the previous case, but with $r_0^{(1)} < r < r_0^{(2)}$. The brane expands from $r = r_0^{(1)}$ to $r = r_0^{(2)}$ at $\lambda = 0$, and contracts again to $r = r_0^{(1)}$.
5. $\mathbf{T}^2 < \mathbf{T}_{\text{crit}}^2$. In this case, as we have already pointed out, the equation $f(r_0) = T^2 r_0^2$ has two solutions, r_0^+ and r_0^- . The brane expands from $r = r_0^-$, emerges from the

horizon, reaches its maximum radius $r = r_0^+$ for $\lambda = 0$, and shrinks again to $r = r_0^-$. This trajectory is completed in a finite amount of proper time, as we will see.

We remark that, as we have pointed out, our Euclidean analysis is feasible only for $T < T_{crit}$, condition needed to have a well-defined preparation time τ_0 . Therefore only the last situation is of interest for our analysis. Nonetheless, a continuously expanding brane with $T > T_{crit}$ (first and third case) implies, from a braneworld cosmology point of view, a 4-dimensional Friedmann universe with a positive cosmological constant, which undergoes for late times a de Sitter expanding phase. This cosmological scenario is clearly more in accordance with the behaviour of our observed universe with respect to the Big Bounce cosmology of the last case. Therefore, an interesting future development of this work could be its extension to over-critical branes, which probably requires a different class of CFT states in the dual theory.

Focusing on the last case, a few final remarks are worth of attention. First, the choice of the sign of the tension T determines which vector normal to the brane we are considering,⁹ i.e. which one of the two sides of the brane we are retaining. The choice $T > 0$ corresponds to a Lorentzian geometry which contains the complete right asymptotic region and part of the left one, ending on the ETW brane (see Figure 1). Additionally, the total brane proper time needed to complete the trajectory from r_0^- to r_0^+ and back is given by

$$\lambda_{tot} = 2 \int_{r_0^-}^{r_0^+} d\hat{r} \frac{1}{\sqrt{T^2 \hat{r}^2 - f(\hat{r})}} \quad (56)$$

and is clearly finite. This expression is the one used in Table 1 in order to quantify the portion of the trajectory of the brane where the adiabatic approximation is reliable. Finally, from the definition of proper time, we find

$$\dot{t} = \frac{dt}{d\lambda} = \pm \frac{Tr}{f(r)}. \quad (57)$$

Referring again to Figure 1, $f(r)$ has a definite (negative) sign in region II ($r_- < r < r_+$). This feature implies that the Schwarzschild time is monotonic with respect to the proper time during the brane trajectory in that region. Thus, if in the contraction phase the brane crossed the outer horizon, for instance, from the left asymptotic region I' (i.e. it crossed the line $r = r_+$, $t = -\infty$), it must cross the inner horizon to the right internal region III (i.e. it must cross the line $r = r_-$, $t = \infty$), cutting off completely the left internal region. As far as we know, this was first noted in ref.⁴² The existence of the minimum radius r_0^- , where the brane reverses again its motion, suggests that, gluing together more spacetime patches as in Figure 1, we can obtain a cyclical Big Bounce cosmology (with the caveat that gravity is not always localized on the brane during the trajectory). However, it is not clear if the effective semiclassical analysis we used to derive the brane trajectory is reliable when the brane is close to or inside the inner horizon. Indeed, the instability of the Cauchy horizon against even small excitations of bulk fields implies that curvature singularities may appear,⁴² preventing a smooth evolution of the brane trajectory.

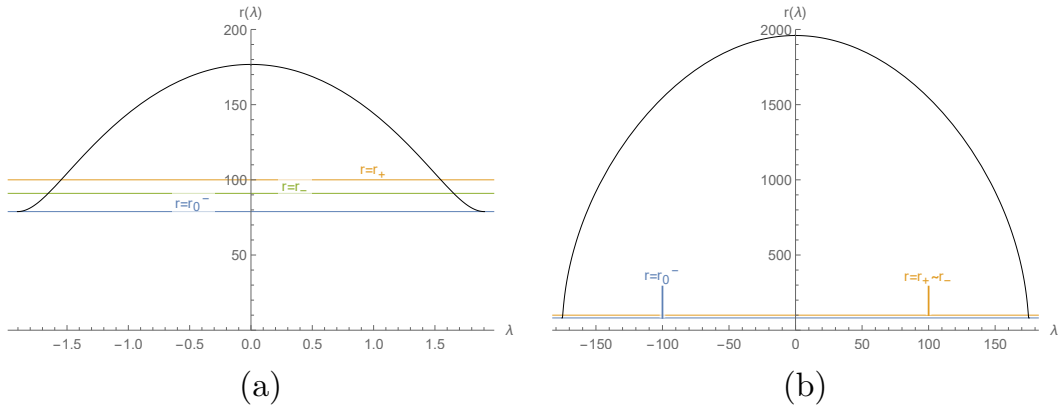


Figure 10: **Proper brane trajectory $r(\lambda)$.** (a) During its trajectory, the brane radius expands to a maximum value $r_0 > r_+$ and shrinks to a minimum value $r_0^- < r_-$. $d = 4$, $r_+ = 100$, $r_- = 91$, $T = 0.89$, $L_{AdS} = 1$. (b) For larger values of the brane tension T , the maximum radius of the brane increases, and the inversion at the minimum radius becomes sharper. $d = 4$, $r_+ = 100$, $r_- = 99.9$, $T = 0.99999$, $L_{AdS} = 1$.

E Gravity Localization and trapping coefficient method

Before clarifying the technical details of the gravity localization analysis, let us qualitatively understand what conditions we expect to be necessary in order to obtain an effective 4-dimensional description of gravity on the ETW brane.

1. The radius of the brane must be much larger than the event horizon size and the AdS radius: $r_b \gg r_+, L_{AdS}$. Since gravity in a 5-dimensional spacetime is unavoidably influenced by the presence of the fifth dimension, a 4-dimensional description of gravity is achievable only in a region where the gravitational effects directed along the fifth dimension and due to the presence of the black hole are weak. If the brane is too close to the black hole horizon, the gravitational attraction of the black hole is strong and a graviton localized on the brane will certainly “leak” in the fifth dimension, eventually falling into the black hole horizon. On the other hand, if the brane is far enough from the black hole horizon and deep in the asymptotically AdS region ($r_b \gg L_{AdS}$), we recover a setup very similar to Randall-Sundrum II (RS II) model, with the brane embedded in a region of the spacetime which is nearly AdS. Thus we can expect to recover, at least locally, gravity localized on the brane. It is somehow surprising that gravity localization is lost if the radius of the brane is too large, as we will see.
2. The time scale of the motion of the brane must be much smaller than the time scale of oscillation of a graviton: $1/H \ll t_o$. This condition is needed to treat the motion of the brane as adiabatic with respect to gravitational perturbations. In other words, under this condition we can consider the brane as effectively static during the propagation of a graviton. As we will see, this assumption turns out to

be pivotal in our analysis. Indeed, in the case of a moving brane, it is non trivial to define a boundary condition for the graviton wavefunction at the position of the brane.

3. $\frac{[r'(t)]^2}{f(r)} \ll f(r)$ or equivalently $\frac{[y'(t)]^2}{f(y)} \ll f(y)$. It is clear looking at the definition of the brane proper time that this condition guarantees that the properties of the graviton are interpreted, up to a constant redshift factor $\sqrt{f(r_b)} = \sqrt{f(y_b)}$, in the same way by a bulk observer (from the perspective of which we develop our analysis) and by an observer comoving with the brane.

We remark that, differently from the AdS-Schwarzschild case, if the black hole is large, the first condition can be satisfied for part of the brane trajectory while still retaining a positive preparation time, provided that the brane is near-critical and the black hole near-extremal. The presence of the black hole unavoidably alters the RS II model, therefore we expect gravity localization to be only a local phenomenon, and valid only for a limited range of time.

E.1 TT perturbations and Schrödinger equation

The first step to find the Schrödinger equation reported in Section 4 is to derive the linearized Einstein equations about the AdS-RN background. Since we are considering only the tensor component of the metric perturbation, the perturbations of the electromagnetic field (which couple only to the scalar and the vector perturbations of the metric⁴³) can be neglected. Therefore, the only terms arising from the perturbation of the electromagnetic stress-energy tensor will be the ones linear in the metric perturbation and with an unperturbed electromagnetic field. For a TT perturbation the linearized Einstein equations read

$$\delta R_{\mu\nu} = \left(\frac{2}{d-1} \Lambda + \frac{(d-2)Q^2}{r^{2d-2}} \right) \delta g_{\mu\nu} \quad (58)$$

with

$$\delta R_{\mu\nu} = -\frac{1}{2} \square_{d+1} \delta g_{\mu\nu} + R_{\rho\mu\sigma\nu} \delta g^{\rho\sigma} - \frac{1}{2} R_{\mu\rho} \delta g_{\nu}^{\rho} - \frac{1}{2} R_{\nu\rho} \delta g_{\mu}^{\rho} \equiv \Delta_L \delta g_{\mu\nu}^{\rho} \quad (59)$$

where \square_{d+1} is the $(d+1)$ -dimensional covariant d'Alembertian, $R_{\mu\nu\rho\sigma}$ is the Riemann tensor and Δ_L is the Lichnerowicz operator.

Introducing the adimensional coordinates discussed in Section 4 (that we will use in the rest of this section), using the explicit expression for the Christoffels and the components of the Riemann and Ricci tensors and defining the covariant Laplacian Δ_{d-1} on the unit $(d-1)$ -sphere, after a long calculation the spatial components (all the other components are identically satisfied) of equation (58) can be recast in the form

$$\begin{aligned} -\frac{1}{f(y)} \partial_t^2 \delta g_{kl} + f(y) \partial_y^2 \delta g_{kl} + \left[f'(y) - \frac{(5-d)f(y)}{y} \right] \partial_y \delta g_{kl} + \frac{1}{y^2} \Delta_{d-1} \delta g_{kl} \\ + 2 \left[\frac{2f(y)}{y^2} - \frac{d-1}{y^2} \right] \delta g_{kl} = \left[\frac{2d}{\gamma^2} - \frac{2(d-2)q^2}{y^{2d-2}} \right] \delta g_{kl}. \end{aligned} \quad (60)$$

We can now decompose the metric perturbation in terms of the tensor harmonics on the unit $(d - 1)$ -sphere (defined in Section 4):

$$\delta g_{kl} = \sum_k y^{\frac{5-d}{2}} \phi_k(\tilde{t}, y) \mathbb{T}_{kl}^{(k)} \quad (61)$$

and introduce the tortoise coordinate $dr^* = dy/f(y)$, in terms of which the horizon of the black hole is mapped to $r^* \rightarrow -\infty$ and the asymptotic boundary to a finite value $r^* = r_\infty^*$. Equation (60) reduces then to a wave equation for each of the modes $\phi_k(\tilde{t}, y)$:

$$-\partial_{\tilde{t}}^2 \phi_k(\tilde{t}, y) = -\partial_{r^*}^2 \phi_k(\tilde{t}, y) + V_k[y(r^*)] \phi_k(\tilde{t}, y) \quad (62)$$

where the potential $V_k[y(r^*)]$ is given by equation (10) and is in accordance with the results of ref.⁴³ In the frequency domain, equation (62) finally takes the form of the Schrödinger equation (9), which encodes the effects of the radial extra dimension on a transverse-traceless graviton.

By finding the expression of the tortoise coordinate r^* as a function of the adimensional radial coordinate y in the limit of large y , it is easy to show that the potential (10) diverges at the asymptotic boundary as $V(r^*) \sim 15/[4(r_\infty^* - r^*)^2]$. This behaviour is very similar to the one typical of the RS II potential.²⁶⁻²⁸ On the other hand, at the black hole horizon ($r^* \rightarrow -\infty$) the potential vanishes exponentially: $V(r^*) \sim \exp(2k_g r^*)$ where k_g is the above defined surface gravity of the black hole. Since the normalizable zero-graviton mode bound on the brane present in the RS II model is a marginally bound mode, and since our potential vanishes exponentially while RS's one exhibited a power-law behavior deep into the bulk, we cannot expect to find a normalizable bound mode as well. But the presence of the brane still allows the existence of a quasi-bound mode, with complex frequency $\omega = \bar{\omega} + i\Gamma/2$, very well localized close to the brane. Its finite lifetime (determined by the imaginary part of the frequency $\Gamma/2$) implies that it will stay on the brane for an interval of time, after which it will eventually leak into the bulk black hole.

Up to this point, we only studied the perturbed Einstein equations, without taking into account the presence of the ETW brane. To study the evolution of a TT graviton living on the brane, and to understand whether or not it is possible for this graviton to remain bound on the brane at least locally and for a reasonable amount of time, we need to enforce a boundary condition for the graviton wavefunction at the position of the brane. At each instant of time, the brane is effectively a hypersurface at fixed y (i.e. at fixed r^*), therefore the previous analysis can be applied to study a gravitational perturbation on the brane. In particular, the Schrödinger equation allows us to understand if the graviton is bound on the brane or if it necessarily leaks into the bulk. If the brane is expanding or contracting, it is not clear how to implement such a boundary condition. But if the time scale of the perturbation is much smaller than the time scale of the motion of the brane, the linearization of equation (5) provides the boundary condition needed. In other words, we must work under an adiabatic approximation for the motion of the brane with respect to the time scale of the perturbation, so that we can approximately consider the ETW brane to be static at $y = y_b$, or $r^* = r_b^*$. Additionally,

since all the calculations will be carried out in the bulk coordinates assuming the brane to be static, in order for an observer comoving with the brane to interpret correctly the graviton, we must also verify that the redshift between the bulk coordinates and the comoving coordinates on the brane is compatible with the assumption of a static brane. From the definition of proper time, this means that $y'^2 \ll f^2(y)$ must hold.

Equation (5) can be traced and rewritten as

$$K_{ab} = \tilde{T}h_{ab} \quad (63)$$

where $\tilde{T} = r_+T$ and the extrinsic curvature is computed using the adimensional coordinates. For a static brane, the normal dual vector is given by $n_\mu = \delta_{\mu,y}/\sqrt{f(y)}$ and $e_a^\mu = \delta_a^\mu$. Linearizing equation (63) and using the decomposition (61) of the metric perturbation, we obtain the boundary condition

$$\partial_y \psi_{k,\omega} \Big|_{y=y_b} = \frac{4\tilde{T}y - (5-d)\sqrt{f(y)}}{2y\sqrt{f(y)}} \psi_{k,\omega} \Big|_{y=y_b}. \quad (64)$$

Using the condition $y'^2 \ll f^2(y)$, equation (6) guarantees that $f(y) \sim \tilde{T}^2 y^2$. The latter result and the definition of the tortoise coordinate finally lead to the boundary condition reported in Section 4, i.e.

$$\partial_{r^*} \psi_{k,\omega} \Big|_{r^*=r_b^*} = \frac{(d-1)\sqrt{f[y(r^*)]}}{2y(r^*)} \psi_{k,\omega} \Big|_{r^*=r_b^*}. \quad (65)$$

As we have already discussed, imposing this boundary condition is equivalent to add to the potential (10) a negative delta term, which “traps” the graviton, allowing gravity localization. Before reviewing the trapping coefficient method introduced in ref.³⁰ and give more details about our numerical results, we remark that in the small black hole case ($\gamma \gtrsim 1$) the potential (10) presents a peak for $r^* \sim 0$ before diverging at $r^* = r_\infty^*$ (see Figure 11). This feature disappears for large black holes. If the brane radius was able to reach values consistently larger than the position of the peak, it would have implied not only the presence of a quasi-bound zero mode, but also the existence of “overtones”³⁰ trapped in the resonance cavity between the peak and the brane position. Nonetheless, as we have already shown, in the small black hole case the ratio between the maximum brane radius and the horizon of the black hole cannot be large, implying that no quasi-bound modes exist. Therefore, the small black hole case is not of our interest and we will focus our attention on the $\gamma \ll 1$ case.

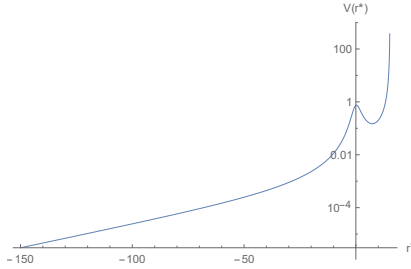


Figure 11: **Potential $V_k[y(r^*)]$ - Small black hole.** $r_+ = 0.1$, $r_- = 0.099$, $L_{AdS} = 1$. The potential diverges for $r_\infty^* = 15.3$ and vanishes exponentially at the horizon $r^* \rightarrow -\infty$. Differently from the large black hole case (see Figure 4), the potential exhibits a peak for $r^* \sim 0$.

E.2 Trapping coefficient method

The quasi-normal modes, already studied in ref.³⁰ for the Schwarzschild-AdS spacetime in the presence of a static brane, are modes with a finite lifetime determined by the imaginary part of the frequency $\Gamma/2$ and purely infalling boundary condition at the black hole horizon, i.e. $\psi_{k,\omega} \sim \exp(i\omega r^*)$ for $r^* \rightarrow -\infty$. This finite lifetime can be understood as a probability of tunneling through the potential barrier from the delta potential at the position of the brane toward the black hole horizon. The absence of the resonant cavity in the potential (10) for the large black hole case implies that only one resonant mode, supported by the attractive delta potential, exists, that we will call quasi-bound mode. Our analysis is based on the trapping coefficient method introduced in ref.,³⁰ that we will review and apply to the AdS-Reissner-Nordström case.

Since the potential vanishes approaching the horizon, the wavefunction in that region must take the form of a plane wave:

$$\psi_{k,\omega}(r^*) \sim \frac{1}{2} A_h e^{-i\delta(\omega)} \left[e^{-i\omega r^*} + S(\omega) e^{i\omega r^*} \right] \quad (66)$$

where $S(\omega) = e^{2i\delta(\omega)}$ is the scattering matrix and $\delta(\omega)$ is the scattering phase shift. The black hole horizon is located at $r^* = -\infty$, and we want purely infalling solutions, therefore in that limit $\psi_{k,\omega}$ must be a left-moving plane wave. Since we are imposing two boundary conditions (equation (65) at the brane and the pure infalling one at the horizon), we expect to find a discrete set of solutions to the Schrödinger equation (the quasi-normal modes), corresponding to a discrete set of frequencies ω_n . By considering complex frequencies, we can obtain the purely infalling solutions by requiring the scattering matrix to have a pole at the quasi-normal mode frequencies ω_n ¹. It can be shown^{30,50} that the leading order Laurent expansion of $S(\omega)$ is given by:

$$S(\omega) \sim e^{2i\delta_0(\omega)} \frac{\omega - \omega_n^*}{\omega - \omega_n} \quad (67)$$

¹In the large black hole case, only one mode, supported by the attractive delta potential, will be present in the spectrum. In the following we will then drop the n index, understood to take the value $n = 0$.

where $\delta_0(\omega)$ is a slowly varying real function of ω . Using the definition $\omega_n = \bar{\omega}_n + i\Gamma_n/2$, the scattering phase shift can be expressed as:

$$\delta(\omega) \sim \delta_0(\omega) + \arcsin \left[\frac{\Gamma_n}{\sqrt{4(\omega - \bar{\omega}_n)^2 + \Gamma_n^2}} \right]. \quad (68)$$

For real ω and if Γ_n is small with respect to $\bar{\omega}_n$, $\delta(\omega)$ varies of a value which is approximately π when ω is varied across the real part of the resonance frequency, flipping the sign of the wavefunction (66). We can now define the trapping coefficient

$$\eta(\omega) \equiv \frac{A_b}{A_h} \quad (69)$$

where A_b is the magnitude of the wavefunction $\psi_{k,\omega}$ at the brane and A_h its magnitude at the horizon of the black hole (effectively, in a region where the potential is almost vanishing). Intuitively, since we expect the quasi-bound mode to be almost localized on the brane due to the presence of the attractive delta potential at $r^* = r_b^*$, the trapping coefficient will present a peak at the frequency of the quasi-bound mode. In the case of a normalizable bound mode (with vanishing imaginary part of the frequency), clearly the wavefunction would vanish at the horizon, giving an infinite trapping coefficient. For a purely infalling solution we can write in general:³⁰

$$\psi_{k,\omega}(r^*) = N(\omega) \begin{cases} A_h \Re [e^{i\delta(\omega)} e^{i\omega r^*}] & r^* \rightarrow -\infty \\ R(\omega) \Re [e^{i\delta(\omega)} e^{i\theta(\omega)}] = -R(\omega) \sin(\delta(\omega) + \theta(\omega) - \frac{\pi}{2}) \equiv A_b & r^* = r_b^* \end{cases} \quad (70)$$

where \Re indicates the real part and $R(\omega)$ and $\theta(\omega)$ are slowly-varying functions of the frequency. For every frequency ω we can choose the normalization $N(\omega)$ of the wavenfunction such that $A_b = 1$, and of course the trapping coefficient will be unchanged. This allows us to set $\psi(r_b^*) = 1$ in our numerical analysis, obtaining:

$$\psi_{k,\omega}(r^*) = \begin{cases} -\frac{A_h}{R(\omega) \sin(\delta(\omega) + \theta(\omega) - \frac{\pi}{2})} \Re [e^{i\delta(\omega)} e^{i\omega r^*}] = -\frac{1}{\eta(\omega)} \Re [e^{i\delta(\omega)} e^{i\omega r^*}] & r^* \rightarrow -\infty \\ 1 & r^* = r_b^* \end{cases} \quad (71)$$

where the trapping coefficient therefore reads:

$$\eta(\omega) = \frac{R(\omega) \sin(\delta(\omega) + \theta(\omega) - \frac{\pi}{2})}{A_h}. \quad (72)$$

If the relation

$$\delta_0(\omega) + \theta(\omega) \sim \frac{\pi}{2}, \frac{3\pi}{2} \quad (73)$$

holds, the square of the trapping coefficient takes the form:

$$\xi(\omega) \equiv \eta^2(\omega) \sim \frac{R^2(\omega)}{A_h^2} \frac{\Gamma_n^2}{4(\omega - \bar{\omega}_n)^2 + \Gamma_n^2}. \quad (74)$$

This Lorentzian (Breit-Wigner) peak is centred at the real part of the frequency of the quasi-bound mode, while its half-width at half-maximum $\Gamma/2$ gives the imaginary part of the frequency, and therefore the lifetime of the mode. If the condition (73) is not satisfied, the shape of the peak is more complicated. Nonetheless, at least for the zero mode of our interest, it has been shown that the condition (73) holds in a good approximation³⁰ and our numerical analysis confirms this result. We mention here the possibility of refining such an approximation by subtracting from the plot of $\xi(\omega)$ as a function of the frequency a baseline function accounting for the slow variation of $\delta_0(\omega)$ and $\theta(\omega)$ with the frequency. For our purposes, such a procedure (which leads to some difficulties due to the arbitrariness of the choice of the baseline³⁰), turns out to be not necessary. It is therefore possible, in a reasonable approximation, to find the real and imaginary parts of the frequencies of the quasi-bound mode (we remind that for the large black hole case we expect only the $n = 0$ mode to be present, supported by the negative delta potential at the position of the brane) using the following procedure (trapping coefficient method):

1. Compute numerically a family of solutions of the Schrödinger equation (9), parameterized by real-valued frequencies ω and with boundary condition (65), requiring also $\psi_{k,\omega}(r_b^*) = 1$;
2. Find numerically the maximum of the wavefunction in the region where the potential is almost vanishing (i.e. near the horizon) for a range of values of ω ;
3. Plot the square of the inverse of these maxima as a function of ω : a peak will be present at the real part of the frequency of the (purely infalling) quasi-normal mode;
4. Eventually subtract a baseline function;
5. Fit the data with the Breit-Wigner distribution (74) to find real and imaginary parts of the frequency of the quasi bound mode.

E.3 Numerical results

We will find the real and imaginary parts of the frequency and the height of the peak R/A_h for three sizes of the black hole: $r_+ = 10, 100, 10000$ (with $L_{AdS} = 1$ and r_- such that the black holes are near extremality), corresponding to $\gamma = 0.1, 0.01, 0.0001$ respectively. For each case we will consider different positions y_b for the brane and values for the angular momentum l . The results of the fits are reported in Table 2.

From our analysis the following picture emerges (we remind that $\gamma = L_{AdS}/r_+$ and $y_b = r_b/r_+$):

- For fixed γ and l , increasing the distance of the brane y_b the real part of the frequency $\bar{\omega}$ decreases and the peak of the square of the trapping coefficient ξ becomes sharper and higher, indicating that the imaginary part of the frequency $\Gamma/2$ decreases as well and gravity localization is more efficient. This is evident

from the data reported in Table 1 (where $t_o = 1/\bar{\omega}$ and $t_d = 2/\Gamma$). But if the brane is very far, $\bar{\omega}$ approaches zero. When it happens, the peak becomes broader (indicating $\Gamma \sim \bar{\omega}$) and is not approximable with a Lorentzian curve anymore. At this point, the peak is very high, indicating a short-lived (large ratio between imaginary and real part of the frequency) but very well localized quasi-bound state. After that, for even farther brane, the quasi-bound mode is no more present (there is no peak, and the trapping coefficient never becomes very big). Additionally, for low values of the angular momentum l , the real part of the frequency obtained is not in accordance with the one expected from a 4-dimensional perturbation of an Einstein static universe (given by $\omega_{GR} = \sqrt{f(y) \cdot (l+2)l}$),³⁰ even when the brane is far and the peak is narrow. For higher values of l instead, i.e. for smaller scale perturbations, the GR expected value and the one obtained numerically are closer. We report here the data showing these behaviors only in the $\gamma = 0.01$ case, but we verified that the same analysis applies also for $\gamma = 0.1, 0.0001$ as well as in the small black hole case. The smaller is the black hole, the farther is the position of the brane where gravity localization is lost. We remark how this behaviour is in contradiction with the conclusions of ref.,³⁰ where it is argued that the real part of the frequency approaches a constant value and the RS II normalizable bound zero-graviton mode is recovered in the far brane limit. However, it is worth noting that the loss of localization for the small black hole case, which is the one mainly studied in ref.,³⁰ occurs for a position of the brane much farther than the ones explored in Figure 11 of ref.³⁰

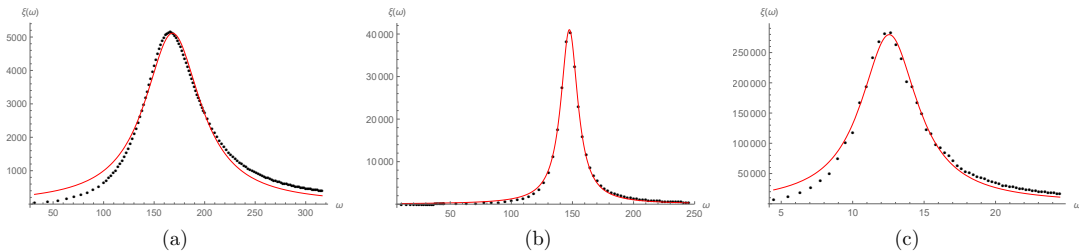


Figure 12: Delocalization for far brane. $d = 4$, $r_+ = 100$, $r_- = 99.9$, $L_{AdS} = 1$, $l = 1$. For fixed black hole size and angular momentum, if the brane is too far from the horizon gravity localization is lost. (a) $y_b = 17.34$. If the brane is not far enough from the horizon, the peak of the squared trapping coefficient is not well approximated by the Lorentzian profile and gravity localization is not very efficient. (b) $y_b = 34.62$. When the brane is farther, gravity localization is more efficient and the peak of the squared trapping coefficient is Lorentzian. (c) $y_b = 66$. If the brane is too far from the horizon, the peak becomes broad, the mode is short-lived and gravity is no more localized.

- For fixed l and y_b , decreasing γ (i.e. increasing the size of the black hole) the real part of the frequency grows and the peak becomes broader, indicating a shorter-lived quasi-bound mode. The Lorentzian approximation of the peak is also less precise. At the same time, we remind that the same maximum radius of the brane

r_0 is reached for a smaller value of the tension T if the black hole is larger.

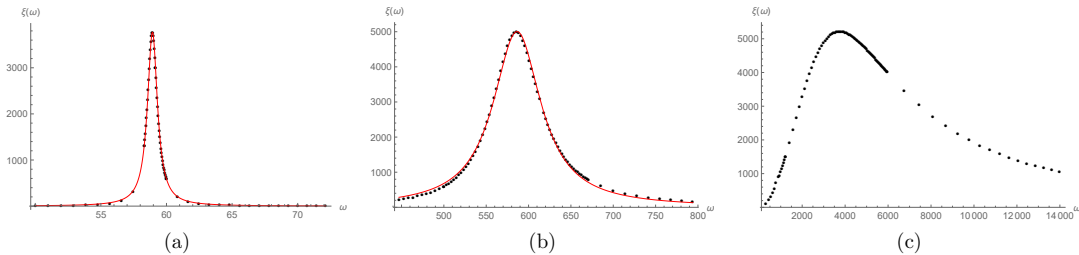


Figure 13: **Delocalization for large black holes.** $d = 4$, $r_-/r_+ = 0.99$, $L_{AdS} = 1$, $y_b = 17.34$, $l = 5$, $\gamma = 0.1$ (a), $\gamma = 0.01$ (b) and $\gamma = 0.001$ (c). Increasing the size of the black hole for fixed angular momentum and radius of the brane, the peak of the squared trapping coefficient is broader and not well approximated by the Lorentzian profile: gravity localization becomes less efficient.

- Holding γ and y_b fixed and increasing the angular momentum l the real part of the frequency grows. In the small black hole case, we verified that the imaginary part of the frequency decreases, exactly how described in ref.³⁰ Differently, in the large black hole case, the imaginary part grows, but much slower than the real part. The peaks are therefore narrower and the ratio between the imaginary and the real part decreases. At the same time, since the imaginary part of the frequency increases, the height of the peaks decreases with increasing l , indicating that, even if they are able to undergo a larger number of oscillations before decaying, these smaller-scale modes have a shorter lifetime than the larger-scale ones (even if localization is still very efficient). These characteristics can be observed comparing the peaks for different values of l in all the three cases, but are particularly evident in the very large black hole cases $\gamma = 0.0001$. We remark that even for a very far brane, which does not support localization of gravity for instance for $l = 1$, increasing the angular momentum the quasi-bound state is recovered. For example, for $\gamma = 0.01$ and $l = 1$ the quasi bound state is lost for $y_b \sim 66$, but for $l = 5$ it is still present when the brane radius is $y_b = 99.94$.

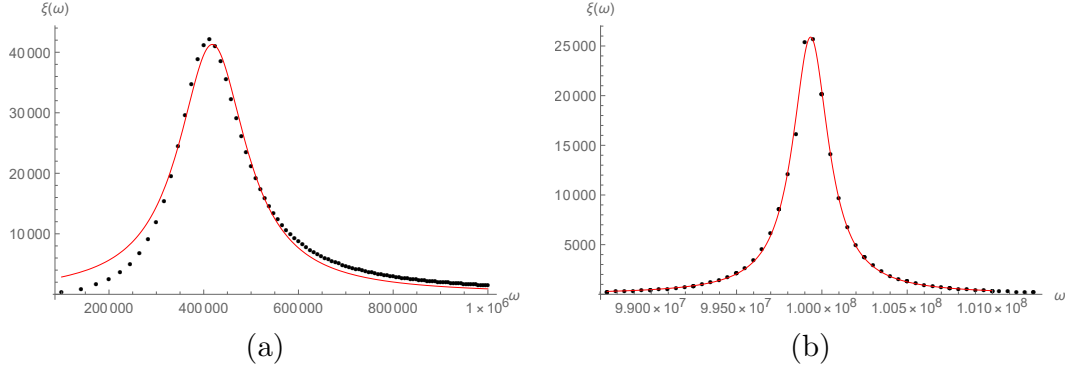


Figure 14: **Localization for small scales.** $d = 4$, $r_+ = 10000$, $r_- = 9900$, $L_{AdS} = 1$, $y_b = 34.62$, $l = 100$ (a) and $l = 10000$ (b). For fixed radius of the brane and size of the black hole, increasing the angular momentum (i.e. decreasing the scale of the perturbation) the peak of the squared trapping coefficient is better approximated by the Lorentzian profile and gravity localization becomes more efficient.

- Keeping the size of the black hole and the scale of the perturbation constant while increasing the brane radius, i.e. increasing l and y_b of the same factor holding γ fixed, the peak becomes narrower and gravity localization more efficient: remaining on a local enough scale, if the brane is farther we are in a setup more similar to the RS II scenario.

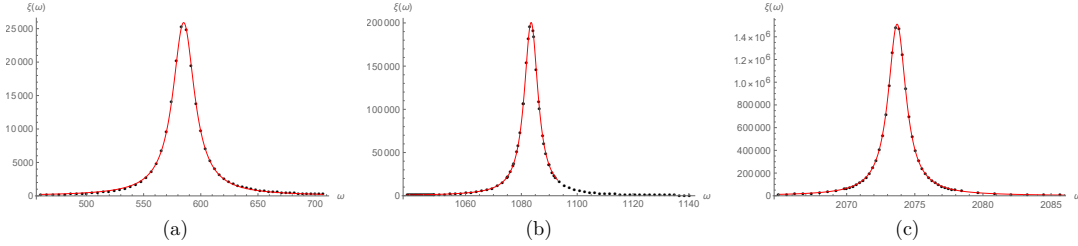


Figure 15: **Localization for far brane and small scales.** $d = 4$, $r_+ = 100$, $r_- = 99.9$, $L_{AdS} = 1$. (a) $l = 5$, $y_b = 30$. (b) $l = 10$, $y_b = 60$. (c) $l = 20$, $y_b = 120$. For fixed black hole size, increasing the angular momentum and the radius of the brane of the same factor, the mode is longer-lived and gravity localization becomes more efficient.

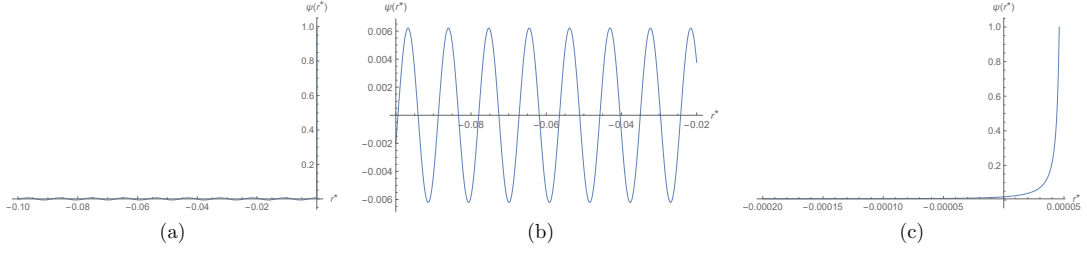


Figure 16: **Example of quasi-bound mode wavefunction.** $d = 4$, $r_+ = 100$, $r_- = 99.9$, $L_{AdS} = 1$, $l = 5$, $y_b = 30$. (a) Quasi-bound mode wavefunction. (b) Detail of the oscillatory behaviour near the horizon. (c) Detail of the growth near the brane.

γ	y_b	l	r_-	R/A_h	$\bar{\omega}$	Γ	ω_{GR}
0.1	17.34	1	9.99	68.22	17.22	0.7354	17.32
0.1	17.34	5	9.99	61.41	58.93	0.9186	59.16
0.01	17.34	1	99.9	71.51	168.2	67.22	173.2
0.01	34.62	1	99.9	202.5	147.5	16.86	173.2
0.01	60.22	1	99.9	464.8	71.70	5.580	173.2
0.01	63	1	99.9	499.2	52.40	5.060	173.2
0.01	66	1	99.9	528.8	12.56	4.835	173.2
0.01	66.15	1	99.9	~ 519.6	~ 4	~ 5	173.2
0.01	17.34	5	99.9	70.74	586.4	68.55	591.6
0.01	30.00	5	99.9	160.9	585.0	23.09	591.6
0.01	34.62	5	99.9	199.5	583.6	17.28	591.6
0.01	99.94	5	99.9	980.9	530.5	2.081	591.6
0.01	60.00	10	99.9	447.8	$1.084 \cdot 10^3$	5.984	$1.095 \cdot 10^3$
0.01	120.0	20	99.9	$1.229 \cdot 10^3$	$2.074 \cdot 10^3$	1.587	$1.095 \cdot 10^3$
0.001	17.34	5	999	~ 73	$\sim 4 \cdot 10^3$	$\sim 5 \cdot 10^3$	$5.916 \cdot 10^3$
0.0001	34.82	100	9900	203.2	$4.181 \cdot 10^5$	$1.737 \cdot 10^5$	$1.010 \cdot 10^6$
0.0001	34.82	1000	9900	180.9	$9.955 \cdot 10^6$	$2.097 \cdot 10^5$	$1.001 \cdot 10^7$
0.0001	34.82	10000	9900	160.9	$9.993 \cdot 10^7$	$2.552 \cdot 10^5$	$1.000 \cdot 10^8$

Table 2: **Quasi-bound modes.** Results of the numerical analysis based on the trapping coefficient method. $L_{AdS} = 1$. The fitted values for $\gamma = 0.01$, $y_b = 66.15$, $l = 1$ and for $\gamma = 0.001$, $y_b = 17.34$, $l = 5$ are purely indicative. We remark that for each set of parameters reported above it is possible to choose a tension T for the brane such that the corresponding y_b is, for instance, the turning point of the brane, while the corresponding Euclidean solutions are sensible ($\tau_0 > 0$) and dominant in the gravity path integral ($\Delta I < 0$).

E.4 Time scales and adiabatic approximation

As we pointed out in Section 4, the three time scales that we must compare in order to verify that the adiabatic approximation we used is reliable are the oscillation time $t_o = 1/\bar{\omega}$, the decay time $t_d = 2/\Gamma$ and the quantity

$$T_H = \frac{y(t)}{y'(t)} = \frac{\tilde{T}y^2}{f(y)\sqrt{\tilde{T}^2y^2 - f(y)}}, \quad (75)$$

which in comoving coordinates would correspond to the Hubble time of the braneworld cosmology, and that we will call for simplicity ‘‘Hubble time’’. If $t_o \ll T_H$ for a given radius of the brane $y = y_b$, the adiabatic approximation holds. We remark that the Hubble time does not depend on the angular momentum l . Thus, since increasing l the real part of the frequency increases and the oscillation time t_o decreases, for higher values of l it is easier to satisfy the adiabatic approximation condition. Additionally, as we have explained, the relation

$$\frac{[y'(t)]^2}{f^2(y)} = \frac{\tilde{T}^2y^2}{\tilde{T}^2y^2 - f(y)} \ll 1 \quad (76)$$

must hold as well at $y = y_b$. We remind that $\tilde{T} = r_+T$. In Section 4 we have shown that, for $l = 10$, $\gamma = 0.01$, $r_+ = 100$, $r_- = 99.9$ and $T = 0.999999999$ it is possible to obtain $t_d \gg T_H \gg t_o$ for a large part of the brane trajectory, meaning that the adiabatic approximation is reliable and that it breaks down (and therefore our analysis loses its meaning) before the graviton leaks into the bulk. Additionally, the condition (76) is satisfied always when the adiabatic approximation holds. For completeness we report in Figure 17 a plot of these quantities as a function of the position of the brane for the data reported in Table 1.

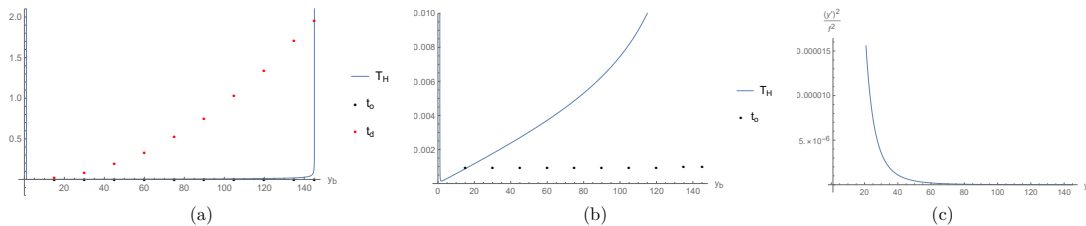


Figure 17: **Time scales comparison for data in Table 1.** $d = 4$, $r_+ = 100$, $r_- = 99.9$, $L_{AdS} = 1$, $l = 10$, $T = 0.999999999$. (a) Hubble time T_H , oscillation time t_o and decay time t_d . (b) Detail of Hubble time T_H and oscillation time t_o only. (c) Ratio $[y'(t)]^2/f^2(y)$. The adiabatic approximation is reliable for at least part of the brane trajectory considered, as discussed in Section 4. The condition $[y'(t)]^2/f^2(y) \ll 1$ is also satisfied.

For the same size and charge of the black hole but with $l = 1$ and $T = 0.99999993325$ (the maximum radius of the brane is $y_0 = r_0/r_+ = 66.15$), using the results reported

in Table 2, we find that the adiabatic approximation is never reliable (i.e. $T_H < t_o$) during the trajectory of the brane (see Figure 18). It clearly holds at the turning point y_0 , where the Hubble time diverges, but there the quasi-bound mode is extremely short-lived ($\bar{\omega}$ and Γ are of the same order). The condition (76) is instead satisfied for a large part of the brane trajectory. This problem sums up with the discordance between the expected 4-dimensional value of the frequency ω_{GR} and the one obtained numerically. Even if for smaller black holes (for instance in the $\gamma = 0.1$ case) close to the turning point the adiabatic approximation can hold also for $l = 1$, we can conclude that an effective 4-dimensional description of gravity localized on the brane is obtained more easily and for a larger amount of brane proper time when the value of the angular momentum l is higher. This result, together with the observation that our analysis is valid only on a time scale smaller than the Hubble time and that the quasi-bound mode is not stable, confirms our expectation to find gravity localization only locally and for a finite amount of time.

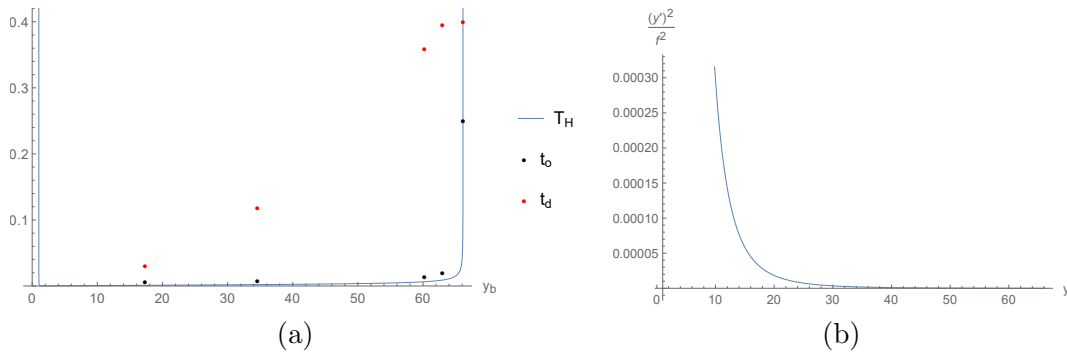


Figure 18: **Time scales comparison for data in Table 2.** $d = 4$, $r_+ = 100$, $r_- = 99.9$, $L_{AdS} = 1$, $l = 1$, $T = 0.99999993325$. (a) Hubble time T_H , oscillation time t_o and decay time t_d . (b) Ratio $[y'(t)]^2/f^2(y)$. The adiabatic approximation is clearly not reliable for the parameters considered. The condition $[y'(t)]^2/f^2(y) \ll 1$ is still satisfied.

References

- [1] Hooft, G. 't. “Dimensional reduction in quantum gravity”. In: *Conf. Proc.* C930308 (1993), pp. 284–296. arXiv: [gr-qc/9310026](#) [[gr-qc](#)].
- [2] Susskind, L. “The World as a hologram”. In: *J. Math. Phys.* 36 (1995), pp. 6377–6396. DOI: [10.1063/1.531249](#). arXiv: [hep-th/9409089](#) [[hep-th](#)].
- [3] Aharony, O. et al. “Large N field theories, string theory and gravity”. In: *Phys. Rept.* 323 (2000), pp. 183–386. DOI: [10.1016/S0370-1573\(99\)00083-6](#). arXiv: [hep-th/9905111](#) [[hep-th](#)].

- [4] Cooper, S. et al. “Black Hole Microstate Cosmology”. In: (2018). arXiv: 1810.10601 [hep-th].
- [5] Karch, A. and Randall, L. “Open and closed string interpretation of SUSY CFT’s on branes with boundaries”. In: *JHEP* 06 (2001), p. 063. DOI: 10.1088/1126-6708/2001/06/063. arXiv: hep-th/0105132 [hep-th].
- [6] Takayanagi, T. “Holographic Dual of BCFT”. In: *Phys. Rev. Lett.* 107 (2011), p. 101602. DOI: 10.1103/PhysRevLett.107.101602. arXiv: 1105.5165 [hep-th].
- [7] Fujita, M., Takayanagi, T., and Tonni, E. “Aspects of AdS/BCFT”. In: *JHEP* 11 (2011), p. 043. DOI: 10.1007/JHEP11(2011)043. arXiv: 1108.5152 [hep-th].
- [8] Kourkoulou, I. and Maldacena, J. “Pure states in the SYK model and nearly- AdS_2 gravity”. In: (2017). arXiv: 1707.02325 [hep-th].
- [9] Almheiri, A., Mousatov, A., and Shyani, M. “Escaping the Interiors of Pure Boundary-State Black Holes”. In: (2018). arXiv: 1803.04434 [hep-th].
- [10] Papadodimas, K. and Raju, S. “An Infalling Observer in AdS/CFT”. In: *JHEP* 10 (2013), p. 212. DOI: 10.1007/JHEP10(2013)212. arXiv: 1211.6767 [hep-th].
- [11] Papadodimas, K. and Raju, S. “State-Dependent Bulk-Boundary Maps and Black Hole Complementarity”. In: *Phys. Rev. D* 89.8 (2014), p. 086010. DOI: 10.1103/PhysRevD.89.086010. arXiv: 1310.6335 [hep-th].
- [12] Papadodimas, K. and Raju, S. “Remarks on the necessity and implications of state-dependence in the black hole interior”. In: *Phys. Rev. D* 93.8 (2016), p. 084049. DOI: 10.1103/PhysRevD.93.084049. arXiv: 1503.08825 [hep-th].
- [13] Harlow, D. “Aspects of the Papadodimas-Raju Proposal for the Black Hole Interior”. In: *JHEP* 11 (2014), p. 055. DOI: 10.1007/JHEP11(2014)055. arXiv: 1405.1995 [hep-th].
- [14] Hartman, T. and Maldacena, J. “Time Evolution of Entanglement Entropy from Black Hole Interiors”. In: *JHEP* 05 (2013), p. 014. DOI: 10.1007/JHEP05(2013)014. arXiv: 1303.1080 [hep-th].
- [15] Binetruy, P., Deffayet, C., and Langlois, D. “Nonconventional cosmology from a brane universe”. In: *Nucl. Phys. B* 565 (2000), pp. 269–287. DOI: 10.1016/S0550-3213(99)00696-3. arXiv: hep-th/9905012 [hep-th].
- [16] Padilla, A. “Brane world cosmology and holography”. PhD thesis. Durham U., 2002. arXiv: hep-th/0210217 [hep-th].
- [17] Gregory, J. P. and Padilla, A. “Exact brane world cosmology induced from bulk black holes”. In: *Class. Quant. Grav.* 19 (2002), pp. 4071–4083. DOI: 10.1088/0264-9381/19/15/313. arXiv: hep-th/0204218 [hep-th].
- [18] Gubser, S. S. “AdS / CFT and gravity”. In: *Phys. Rev. D* 63 (2001), p. 084017. DOI: 10.1103/PhysRevD.63.084017. arXiv: hep-th/9912001 [hep-th].

- [19] Savonije, I. and Verlinde, E. P. “CFT and entropy on the brane”. In: *Phys. Lett.* B507 (2001), pp. 305–311. DOI: 10.1016/S0370-2693(01)00467-1. arXiv: hep-th/0102042 [hep-th].
- [20] Biswas, A. K. and Mukherji, S. “Holography and stiff matter on the brane”. In: *JHEP* 03 (2001), p. 046. DOI: 10.1088/1126-6708/2001/03/046. arXiv: hep-th/0102138 [hep-th].
- [21] Verlinde, E. P. “On the holographic principle in a radiation dominated universe”. In: (2000). arXiv: hep-th/0008140 [hep-th].
- [22] McFadden, P. and Skenderis, K. “Holography for Cosmology”. In: *Phys. Rev.* D81 (2010), p. 021301. DOI: 10.1103/PhysRevD.81.021301. arXiv: 0907.5542 [hep-th].
- [23] Bernardo, H. and Nastase, H. “Holographic cosmology from d -dimensional reduction” of $\mathcal{N} = 4$ SYM vs. $AdS_5 \times S^5$. In: (2018). arXiv: 1812.07586 [hep-th].
- [24] Dong, X., Silverstein, E., and Torroba, G. “De Sitter Holography and Entanglement Entropy”. In: *JHEP* 07 (2018), p. 050. DOI: 10.1007/JHEP07(2018)050. arXiv: 1804.08623 [hep-th].
- [25] Bilic, N. “Randall-Sundrum versus holographic cosmology”. In: *Phys. Rev.* D93.6 (2016), p. 066010. DOI: 10.1103/PhysRevD.93.066010. arXiv: 1511.07323 [gr-qc].
- [26] Randall, L. and Sundrum, R. “Large Mass Hierarchy from a Small Extra Dimension”. In: *Phys. Rev. Lett.* 83 (17 1999), pp. 3370–3373. DOI: 10.1103/PhysRevLett.83.3370. URL: <https://link.aps.org/doi/10.1103/PhysRevLett.83.3370>.
- [27] Randall, L. and Sundrum, R. “An Alternative to Compactification”. In: *Phys. Rev. Lett.* 83 (23 1999), pp. 4690–4693. DOI: 10.1103/PhysRevLett.83.4690. URL: <https://link.aps.org/doi/10.1103/PhysRevLett.83.4690>.
- [28] Karch, A. and Randall, L. “Locally localized gravity”. In: *JHEP* 05 (2001). [,140(2000)], p. 008. DOI: 10.1088/1126-6708/2001/05/008. arXiv: hep-th/0011156 [hep-th].
- [29] Seahra, S. S., Clarkson, C., and Maartens, R. “Delocalization of brane gravity by a bulk black hole”. In: *Class. Quant. Grav.* 22 (2005), pp. L91–L102. DOI: 10.1088/0264-9381/22/16/L02. arXiv: gr-qc/0504023 [gr-qc].
- [30] Clarkson, C. and Seahra, S. S. “Braneworld resonances”. In: *Class. Quant. Grav.* 22 (2005), pp. 3653–3688. DOI: 10.1088/0264-9381/22/17/020. arXiv: gr-qc/0505145 [gr-qc].
- [31] Dias, G. A. S. and Lemos, J. P. S. “Hamiltonian thermodynamics of d -dimensional ($d \geq 4$) Reissner-Nordstrom anti-de Sitter black holes with spherical, planar, and hyperbolic topology”. In: *Phys. Rev.* D79 (2009), p. 044013. DOI: 10.1103/PhysRevD.79.044013. arXiv: 0901.0278 [gr-qc].

- [32] Huang, Y., Liu, D.-J., and Li, X.-Z. “Superradiant instability of D -dimensional Reissner-Nordström-anti-de Sitter black hole mirror system”. In: *Int. J. Mod. Phys. D* 26.13 (2017), p. 1750141. DOI: 10.1142/S0218271817501413. arXiv: 1606.00100 [gr-qc].
- [33] Avelino, P. P. et al. “Mass inflation in a D dimensional Reissner-Nordström black hole: a hierarchy of particle accelerators?” In: *Phys. Rev. D* 84 (2011), p. 024019. DOI: 10.1103/PhysRevD.84.024019. arXiv: 1105.4434 [gr-qc].
- [34] Sadeghi, J. and Reza Shajiee, V. “Quantum Tunneling from the Charged Non-Rotating BTZ Black Hole with GUP”. In: *Eur. Phys. J. Plus* 132.3 (2017), p. 132. DOI: 10.1140/epjp/i2017-11432-x. arXiv: 1605.04595 [hep-th].
- [35] Gouteraux, B. “Black-Hole Solutions to Einstein’s Equations in the Presence of Matter and Modifications of Gravitation in Extra Dimensions”. PhD thesis. Orsay, LPT, 2010. arXiv: 1011.4941 [hep-th].
- [36] Ghosh, A. and Mitra, P. “Temperatures of extremal black holes”. In: (1995). arXiv: gr-qc/9507032 [gr-qc].
- [37] Andrade, T. et al. “Entanglement and correlations near extremality: CFTs dual to Reissner-Nordström AdS_5 ”. In: *JHEP* 04 (2014), p. 023. DOI: 10.1007/JHEP04(2014)023. arXiv: 1312.2839 [hep-th].
- [38] Hawking, S. W. and Ross, S. F. “Duality between electric and magnetic black holes”. In: *Phys. Rev. D* 52 (10 1995), pp. 5865–5876. DOI: 10.1103/PhysRevD.52.5865.
- [39] Chamblin, A. et al. “Charged AdS black holes and catastrophic holography”. In: *Phys. Rev. D* 60 (6 1999), p. 064018. DOI: 10.1103/PhysRevD.60.064018.
- [40] Burikham, P. and Promsiri, C. “The Mixed Phase of Charged AdS Black holes”. In: *Adv. High Energy Phys.* 2016 (2016), p. 5864672. DOI: 10.1155/2016/5864672. arXiv: 1408.2694 [hep-th].
- [41] Chavanis, P.-H. “Cosmology with a stiff matter era”. In: *Phys. Rev. D* 92.10 (2015), p. 103004. DOI: 10.1103/PhysRevD.92.103004. arXiv: 1412.0743 [gr-qc].
- [42] Hovdebo, J. L. and Myers, R. C. “Bouncing brane worlds go crunch!” In: *JCAP* 0311 (2003), p. 012. DOI: 10.1088/1475-7516/2003/11/012. arXiv: hep-th/0308088 [hep-th].
- [43] Kodama, H. and Ishibashi, A. “Master equations for perturbations of generalized static black holes with charge in higher dimensions”. In: *Prog. Theor. Phys.* 111 (2004), pp. 29–73. DOI: 10.1143/PTP.111.29. arXiv: hep-th/0308128 [hep-th].
- [44] Ryu, S. and Takayanagi, T. “Holographic derivation of entanglement entropy from AdS/CFT”. In: *Phys. Rev. Lett.* 96 (2006), p. 181602. DOI: 10.1103/PhysRevLett.96.181602. arXiv: hep-th/0603001 [hep-th].
- [45] Hubeny, V. E., Rangamani, M., and Takayanagi, T. “A Covariant holographic entanglement entropy proposal”. In: *JHEP* 07 (2007), p. 062. DOI: 10.1088/1126-6708/2007/07/062. arXiv: 0705.0016 [hep-th].

- [46] Maldacena, J. and Qi, X.-L. “Eternal traversable wormhole”. In: (2018). arXiv: 1804.00491 [hep-th].
- [47] Cottrell, W. et al. “How to Build the Thermofield Double State”. In: *JHEP* 02 (2019), p. 058. DOI: 10.1007/JHEP02(2019)058. arXiv: 1811.11528 [hep-th].
- [48] Martyn, J. and Swingle, B. “Product Spectrum Ansatz and the Simplicity of Thermal States”. In: (2018). arXiv: 1812.01015 [cond-mat.str-el].
- [49] Yale, A. “Simple counterterms for asymptotically AdS spacetimes in Lovelock gravity”. In: *Phys. Rev. D* 84 (2011), p. 104036. DOI: 10.1103/PhysRevD.84.104036. arXiv: 1107.1250 [gr-qc].
- [50] Taylor, J. R. *Scattering Theory*. New York: Wiley, 1972.